2024-05-01

Sulfonated Polyethersulfone Membranes For Electrodialysis Desalination And The Influence Of Solvent Evaporation On Current Efficiency, Salinity Reduction, And Permselectivity

Li Chen
University of Texas at El Paso

SULFONATED POLYETHERSULFONE MEMBRANES FOR ELECTRODIALYSIS DESALINATION AND THE INFLUENCE OF SOLVENT EVAPORATION ON CURRENT EFFICIENCY, SALINITY REDUCTION, AND PERMSELECTIVITY

LI CHEN

Doctoral Program in Environmental Science and Engineering

APPROVED:

XiuJun (James) Li, Ph.D., Chair

W. Shane Walker, Ph.D.

Eva M Deemer, Ph.D.

Malynda A. Cappelle, Ph.D.

Tweedie Craig E, Ph.D.

Stephen L. Crites, Jr., Ph.D.
Dean of the Graduate School

Dedication

This dissertation is dedicated to the research and application of electrodialysis desalination for the benefit of all human nations to mitigate freshwater scarcity. I also want to dedicate this significant achievement to everyone who supports me physically, emotionally, and spiritually.

SULFONATED POLYETHERSULFONE MEMBRANES FOR ELECTRODIALYSIS DESALINATION AND THE INFLUENCE OF SOLVENT EVAPORATION ON CURRENT EFFICIENCY, SALINITY REDUCTION, AND PERMSELECTIVITY

by

LI CHEN, MA.Eng.

DISSERTATION

Presented to the Faculty of the Graduate School of

The University of Texas at El Paso

in Partial Fulfillment

of the Requirements

for the Degree of

DOCTOR OF PHILOSOPHY

Environmental Science and Engineering Program

THE UNIVERSITY OF TEXAS AT EL PASO

December 2023

Acknowledgements

It can never be possible to do anything without the help and support from different aspects and sources. Especially to complete the PhD education, the highest degree one can achieve in one's whole life. I am not an exception. I thank those who helped and supported me in completing my Doctor of Philosophy program in Environmental Science and Engineering (ESE) at the University of Texas at El Paso (UTEP), Texas, USA.

First, I would like to give thanks to my research group. Great thanks to Dr. Walker, who is an expert in electrodialysis desalination. He gave me advice for my electrodialysis research and experiments and helped a lot to improve my dissertation writing especially in the final stage. And great thanks to the fundings came from him, which supported my PhD study and my family so much during this most difficult period in my life. Also, I feel grateful that he is a dear Brother in the Lord, who often used his spiritual power to pray for me and my family so that I can be strengthened to continue and finish this PhD long-run. Great thanks to my supervisor, the chair of my committee members, Dr. James Li, who is a responsible and reliable professor and advisor. Because of him, I can get admitted to UTEP to pursue a PhD degree in education. Also, in my last stage, which is also the most crucial stage of my education, he graciously stood up to take the responsibility with all his support, super high efficiency, and positive response, to assist me to graduate and achieve success so that I can finish the last run of my Ph.D. education—great gratitude to him. Great thanks to Dr. Deemer, who is an expert in material science. She gave me the most direct direction on membrane synthesis and supported the necessary materials and equipment for the progress of my dissertation research. Especially in the last stage of my education, she stood with me as a superhero to handle all problems including things within my research but also things outside of my research and helped to coordinate with everyone for my academic success.

I am grateful for her precious and close support. Lastly, great thanks and rememorizes to my other lab mates, Martin, Marcela, Beto, Tayia, Hyder, Shahrouz, etc., thanks for your companies that I can have an excellent study time.

Second, I thank the Nanotechnology Enabled Water Treatment (NEWT) center, supported by NSF, for their financial support and opportunities to collaborate with other researchers and colleagues from Rice, Yale, and ASU Universities. Especially in the last stage of my education, I was luckily approved for the NSF internship supplement program through NEWT from NSF. This internship supplement funding makes me available to intern at Carollo Engineers, a consulting company in the water treatment area. With this internship funding, I am grateful to Joe Feuille and Maria Placencia, who worked hard to resolve the funding release to my account. Without their hard work on my complicated case, I cannot continue and finish my research at a peaceful pace.

Thirdly, I would like to thank Dr. Carig E. Tweedie, the director of the ESE program, who was so generous and ready for help and support to my graduation and Ms. Lina Hamdan, the coordinator of the ESE program. Thanks for all your support provided for the completion of my PhD graduation.

I would also like to thank my family members and all the supporting ones. Thanks to my wife, Yingying Sun, for the past four years and a half for her continuous company and support. Thanks to my parents and parents-in-law, with their financial support, we can go through all the financial difficulties. Thanks to my kids, Olivia, and Gloria, you are sweet gifts granted to me by my God. Also, thanks to my master's advisor, Xiangrong Zhu, who is so supportive and enthusiastic about my study abroad. Great thanks and appreciation to saints in the church. Thanks for your spiritual prayer and concern for my research and family during this education period.

Lastly, thanks to my Lord Jesus, my good shepherd. Thanks to my heavenly Father, who took care of us in a secret way. Thanks to the Spirit who dwelled in me and supported me daily closely. Great appreciation and praise to the Triune God!

Abstract

The high cost of ion exchange membranes significantly limits the public application of electrodialysis. The research of novel, inexpensive ion exchange membranes is essential to developing and applying electrodialysis desalination technology. This research focuses on fabricating cation exchange membranes with polyethersulfone (PES) and sulfonated PES (sPES) for water treatment. N-Methyl-2-Pyrrolidone (NMP) was used as an organic solvent to dissolve PES. After different solvent evaporation times were optimized from 0 hr to 24 hr, those membranes were formed through the phase inversion technique. The performance results show that the PES membranes performed the best when the solvent evaporated at 3 hr, while sPES membranes performed the best when the solvent evaporated within 1 hr. The electrodialysis (ED) test results were evaluated with different running conditions such as voltages, flow velocities, and feed solutions. LabVIEW software was used to collect data, including voltage, current, conductivity, etc. Compared with commercial Neosepta cation exchange membranes under the same test conditions, the salinity reduction rates performance of fabricated PES and sPES membranes are approximately 40% and 60% of Neosepta commercial membranes, respectively. Finally, the two membrane combinations with fabricated PES and sPES membranes have a relative transport number (RTN) of SO_4^{2-}/Cl^- both around 0.1; this is probably due to the co-ion transport through fabricated CEMs. The developed membranes have great potential in cost-effective desalination to address the global water crisis.

Keywords: Electrodialysis, desalination, ion exchange membrane, polyethersulfone, sulfonation, NaCl solution, real brackish water, membrane selectivity.

Table of Contents

List of Tables

List of Figures

Chapter 1: General Introduction

1.1 BACKGROUND

Access to safe, drinkable water is one of the most significant limiting factors for the sustainability of human society. Approximately 71% of the Earth's surface is water-covered, and the oceans hold 96.5% of all Earth's water (White, 1993). The fraction of freshwater is only 3.5%, and of that freshwater portion, 68.7% of freshwater is from ice caps, glaciers, and permanent snow, which is not easily accessed (White, 1993). As societies continue to develop, the demand for improved living conditions requires more and more freshwater supply, exacerbating the water scarcity situation. Especially in regions with little access to fresh water like rivers or lakes, brackish groundwater and seawater are increasingly essential water sources. Thus, desalination, which is the process of removing dissolved minerals from saline water, will be an increasingly important method to solve water scarcity challenges across the globe.

Since the application of desalination processes and related technologies, the global desalination capacity has increased non-linearly with time; according to Eke et al. (2020), global installed desalination capacity has been compounding steadily at the rate of 7% per year from 2010 to 2019. According to Desaldata from Global Water Intelligence, in mid-February 2020, the global installed and cumulative desalination capacities for freshwater production were 97.2 million m^3/day and 114.9 million m^3/day, respectively.

Many innovations and technologies have been developed for desalination, and they are generally divided into two categories: membrane desalination and thermal desalination. Specifically, the membrane desalination category includes reverse osmosis (RO) (Fritzmann et al., 2007), electrodialysis (ED), membrane distillation (MD) (Alklaibi & Lior, 2005), capacitive

deionization (CDI) (Oren, 2008), and forward osmosis (FO) (Akther et al., 2015).

Compared with CDI, ED is more energy efficient. According to the research of Patel et al., the energy efficiency performances of CDI and ED were compared in an equivalent background. The results indicated that the energy efficiency of ED often exceeds 30% and is nearly an order of magnitude greater than CDI (Patel et al., 2020). RO is the most widely-utilized membrane desalination technology, with 69% share of the installed desalination capacity (Eke et al., 2020). While ED presently has a small share in low-salinity desalination applications, it is becoming a research hotspot due to its advantage of high-water recovery without requiring phase change, reaction, or chemicals (Al-amshawee et al., 2020). Furthermore, the opportunity to tailor ion selectivity in ion exchange membranes is very auspicious. Compared with MD, although MD process has been known for almost 50 years, it is still at the research and development level, not fully developed yet. Moreover, membrane pore wetting fouling due to salt deposition has been a great challenge for MD (Elsaid et al., 2020). However, ED is more mature than MD, that ED has a share of 2% of the global desalination capacity from a thousand desalination plants (Jones et al., 2019).

1.2 OVERVIEW OF ELECTRODIALYSIS PROCESS

The concept of ED was first proposed in 1890 by Maigrot and Sabates. However, the first synthetic ion-exchange membranes were manufactured in 1950 by W. Juda and W.A. McRay and were used in 1954 to build the first ED desalination plant for Aramco (Saudi Arabia) (Grebenyuk & Grebenyuk, 2002). In 1974, there was a significant breakthrough with the development of the electrodialysis reversal concept (EDR) (Reahl, 2006). At the time of this writing, many “ED-derived” alternatives and applications have been developed, reinforcing the general development of electro-membrane technologies.

ED is an electrically driven process. As shown in Figure 1.1, ED usually comprises a series of ion-exchange membranes (IEMs), including cation exchange membranes (CEMs) and anion exchange membranes (AEMs), alternating concentrate and dilute solution channels, and electrodes at the two ends (Campione et al., 2018).

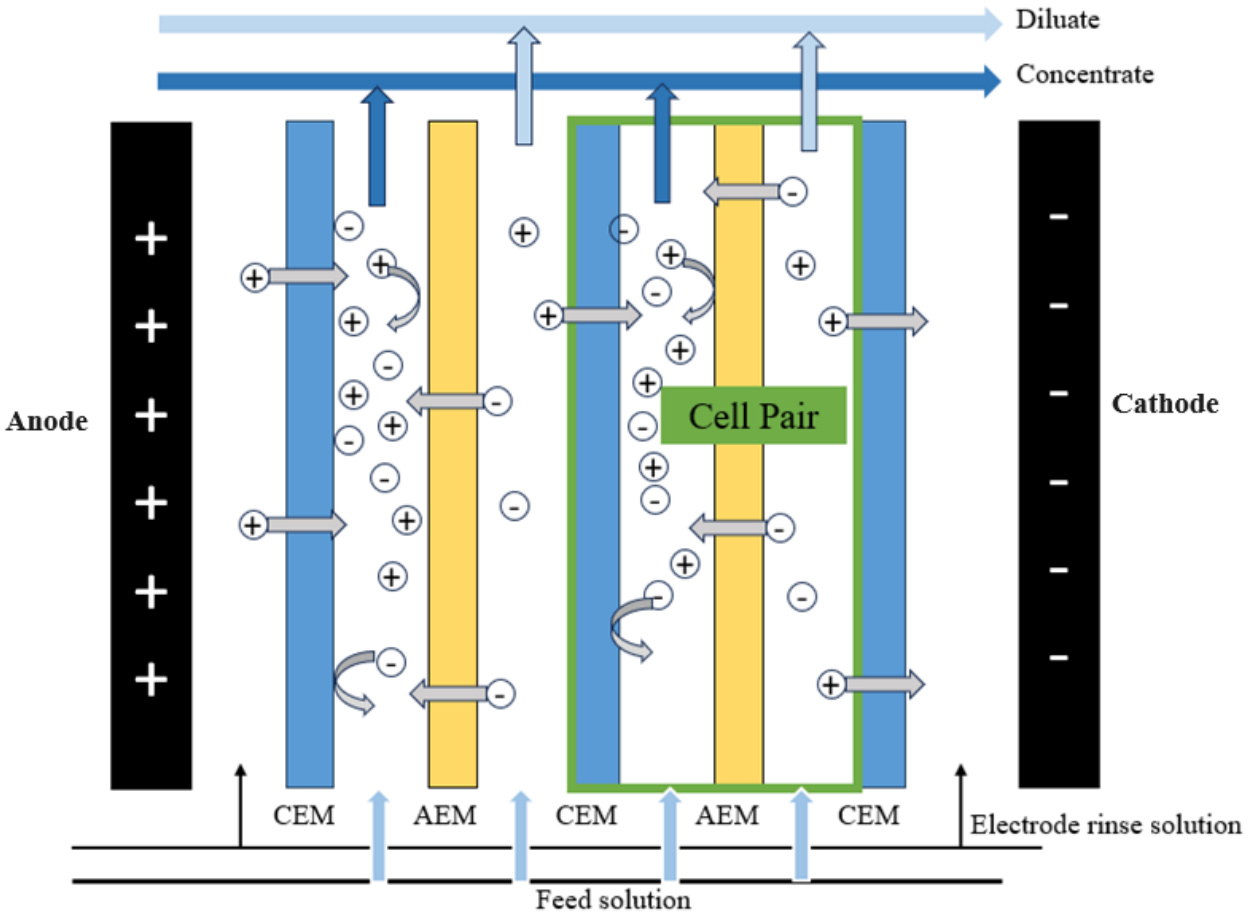

Figure 1.1: Schematics of an electrodialysis system, identifying the repeating unit (cell pair).

IEMs are the critical components of all electro-membrane processes. Thus, developing inexpensive IEMs will significantly facilitate the application of ED technology. The lower market share of ED is mainly due to the relatively high cost of IEMs compared to RO membranes and the significant reduction of membrane selectivity when seawater is used as a feed solution (Campione

et al., 2018) Hence, for the broad application of ED, it is essential to develop cost-effective and high perm-selective IEMs.

1.3 CURRENT DEVELOPMENT OF ION EXCHANGE MEMBRANES

The fabrication of ion exchange membranes is a complex process. For the fabrication methods, traditionally, casting is the most popular way to fabricate IEMs, followed by the technique of phase inversion (Li et al., 2016; Sinha & Purkait, 2015; Thakur & Malmali, 2022; Yun et al., 2006). Casting is the process to spread casting solution onto a flat surface or support to form a thin film. Phase inversion is a way to form membranes by the change of phase, like immersing the wet film in a non-solvent bath to form a solid membrane. Also, hot-press is another way to fabricate IEMs (Krishna et al., 2021). Traditionally, either the fabricating materials or the fabricating processes can have adverse environmental impacts, such as Neosepta commercial IEMs with Nafion, which produce per- and polyfluoroalkyl substances (PFAS). Furthermore, many organic solvents such as benzene, chloroform, carbon tetrachloride, methylene chloride (dichloromethane), and tetrachloroethylene (perchloroethylene) etc., which are carcinogenic to human health and can pollute the environment, are used during the fabrication process (Avci et al., 2020; Di Virgilio et al., 2023). Thus, more environmentally friendly ("greener") fabrication of IEMs is also encouraged in recent years. Some researchers tested the use of chitosan as the fabricating material (Ryu et al., 2019), which is argued to be very environmental-friendly. Some tried green fabrication process without using organic solvent. According to the research of Yang et al. (2019) green fabrication of pore-filling anion exchange membranes (PAEMs) using roll-to-roll (R2R) equipment was conducted. Key methods involved optimizing process parameters like pretreatment time, impregnation time, water amount, and photo-polymerization rate. The results showed that industrial-scale PAEM could be fabricated rapidly and efficiently without using toxic

organic solvents. PAEMs exhibited comparable ion-exchange capacity, resistance, and permselectivity to handmade versions and demonstrated higher power density than commercial ion exchange membranes in reverse electrodialysis (RED) applications. Further research could focus on refining the green fabrication process to enhance the efficiency and scalability of PAEM production. (Yang et al., 2019).

Besides the fabrication of IEMs, researchers also show great interest in improving membrane performance, especially selectivity. Generally speaking, there are two strategies to improve membrane selectivity: one is to adjust a membrane's hydrophobicity; the other is to regulate the compactness of a membrane through post-treatments, including heat treatment and surface modification (Wang et al., 2020). According to the study by Mubita et al. (2020) , it was demonstrated that the selective transport of specific ions across IEMs can be enhanced by controlling membrane properties such as hydrophobicity. The research by Irfan et al. (2020), designed and fabricated novel monovalent cations perm-selective membranes (MCPMs) with hydrophobic alkyl spacers and zwitterion structure, which enabled high monovalent/divalent cation selectivity, reaching up to 25.26 for Na^{+}/ Mg^{2+}. Other researchers have tried to coat original membranes with polyelectrolyte multilayers (Cheng et al., 2014; Jain et al., 2019; Liao et al., 2019; White et al., 2015, 2016; Xu et al., 2018) or layer-by-layer modification with aliphatic polyamide (Abdu et al., 2014; Ahmad et al., 2019), and achieved a significant enhancement of the monovalent/divalent selectivity. Other studies have tested the efficacy of modifying IEMs with a positively or negatively charged layer (Afsar et al., 2019; Radmanesh et al., 2019; Vaselbehagh et al., 2015) or adjusting charge density on functional layers (Pang et al., 2020) to improve membrane selectivity.

The research on membrane selectivity is necessary and has practical value. Researchers

have used monovalent selective membranes to treat greenhouse wastewater for reuse (Ahdab et al., 2021), remove harmful nitrate and fluoride ions from feed solutions (Takagi et al., 2014), and recover lithium from salt-lake brines (Nie et al., 2017) etc. Recently, the most valuable application of monovalent selective ED is to treat groundwater for irrigation, which allows for the removal of chloride and sodium while preserving most hardness ions (Ahdab et al., 2021; Cohen et al., 2018).

Besides the research and improvement of the ion exchange membrane selectivity, researchers have also performed many studies to build modelling of the ED system. According to the research performed by Biesheuvel et al. (2021), who recently published a RO and ED tutorial review. In this review, they presented theory for RO and ED to explain how both technologies are based on fundamental transport theory and illustrate their application in simple geometries, complete modules, and system optimization of multiple combined units. For ED specifically, they developed new equations for Donnan equilibrium that extended the standard ideal expression. ED concentration polarization has a small effect when salt removal is below 80%. Also, most researchers only considered a binary solution component (Moon et al., 2004; H. Zhu et al., 2020; Zourmand et al., 2015), which is irrelevant for most practical applications. However, according to the research of Generous et al. (2020), the sodium chloride binary model could be used for the seawater ED model. In contrast, the multi-component ED model is preferred for brackish water. Recently, there has been a growing consideration of utilizing a multi-component aqueous system in modelling (Honarparvar & Reible, 2020; Rehman et al., 2019). Some researchers have developed modelling for the monovalent selective electrodialysis (MSED) to predict perm-selectivity across different salinities and compositions (Rehman et al., 2021).

1.4 COST ANALYSIS OF ION EXCHANGE MEMBRANES

Even though many studies have been performed to improve the membrane selectivity of

IEMs, and ED modeling has been developed, the high cost of IEMs is still a key factor preventing the wide application of IEMs. According to the published papers, the average cost of IEMs is approximately $100 per square meter (Generous et al., 2021; Lee et al., 2002; Strathmann, 2004). Thus, ED membranes are very expensive compared to RO in which the average membrane cost is approximately $14 per square meter (Pérez et al., 2022); thus, there is a great market opportunity for ED by decreasing the cost of IEMs.

Published literature on the cost analysis of IEM fabrication is limited, especially regarding the cost of IEMs for ED desalination in recent years. According to the research by Pushkareva et al. (2020) a comparative study of anion exchange membranes for low-cost water electrolysis was provided. It assessed the performance of these membranes under different conditions, such as varying KOH concentrations and temperatures. The study emphasized the influence of factors like membrane resistance, electrolyte concentration, catalyst layer structure, and binder type on the overall performance of the electrolysis process. A notable outcome was that Sustainion®-based membrane electrode assemblies (MEAs) showed the best performance across all tested conditions. The research also highlighted the safety of AEM electrolysis technology, especially regarding hydrogen crossover, compared to polymer electrolyte membrane (PEM) technology. Further investigations were suggested to improve MEA structures by exploring different binder types and their compatibility with AEMs.

According to the research of Hand et al. (2019), a technoeconomic analysis (TEA) of brackish water for capacitive deionization was performed, considering the tradeoffs among performance, lifetime, and material costs. It presented a detailed study on the cost and performance of brackish water desalination using capacitive deionization (CDI). It evaluated the capital and operating costs of CDI systems at a large scale, considering both conventional CDI and membrane

CDI (MCDI) with different ion-exchange membrane (IEM) costs. The study revealed that while MCDI typically outperforms CDI, the cost-effectiveness of MCDI was heavily influenced by the price of IEMs. Additionally, the research underscored the importance of system lifetimes in determining the overall cost of water production. The sensitivity of system costs to various operational and material parameters was also assessed, offering insights into the economic viability of CDI systems for brackish water desalination. Specifically, the capital costs were estimated to be 2 to 14 times greater than the operating costs. The study underscored the impact of IEMs prices on the cost-effectiveness of membrane capacitive deionization (MCDI) systems and highlighted the crucial role of achieving system lifetimes of at least two years to optimize the economics. This research presented an example of cost analysis of IEMs, while it was applied on capacitive deionization rather than ED desalination area.

According to the research of Mayyas et al. (2019), a manufacturing cost analysis for proton exchange membrane (PEM) water electrolyzers was performed. It analyzed detailed cost modeling for key components such as the catalyst-coated membrane (CCM), porous transport layer (PTL), and stack assembly. The paper concluded that significant cost reductions in PEM electrolyzer stacks can be achieved through high throughput automated processes, with estimates suggesting a reduction to $125/kW for a production volume of 100 MW, and further to $90/kW at higher volumes. Direct material costs, especially for the catalyst coated membrane, dominated at high production volumes. Balance-of-plant costs represented a major portion of overall system costs, with economies of scale offering substantial cost reductions. Crucially, the cost of hydrogen production via water electrolysis was heavily influenced by electricity prices and electrolyzer capital costs, indicating that reductions in these areas were key to lowering overall hydrogen

generation costs.

Also, according to the research of Chakraborty et al., (2020) a low-cost proton exchange membrane for application in microbial fuel celles was fabricated. It investigated the development and application of a novel, low-cost proton exchange membrane (PEM) synthesized from sulphonated biochar derived from food waste. This PEM, named SBC-600, demonstrated significant cost advantages and comparable performance to traditional Nafion membranes in microbial fuel cell (MFC) applications. The research highlighted the potential of SBC-600 in enhancing the economic feasibility of MFCs for wastewater treatment and renewable energy production. The findings suggested that sulphonated biochar was a promising material for PEMs, offering a sustainable and cost-effective alternative to conventional membranes.

In summary, the cost analysis of IEMs in other applications ranged from 20 to 100 $/m^2 (Chakraborty et al., 2020; Hand et al., 2019; Mayyas et al., 2019; Pushkareva et al., 2020), but there is no such analysis for ED applications for brackish desalination. Also, many researchers conducted membrane performance tests with synthetic binary (*e.g.*, sodium chloride) solutions rather than real brackish water (Chen et al., 2020; He et al., 2016; Khan et al., 2017; Wu et al., 2021). There is a need for research with real brackish water.

1.5 GOALS AND OBJECTIVES OF RESEARCH

The goal of this research is to explore the fabrication of cost-effective ion-exchange membranes for electrodialysis desalination. Low-cost polyether sulfone (PES) is used as the main fabrication material, and different solvent evaporation times are researched to achieve optimized membranes. Additionally, real brackish water is used in the research for the electrodialysis performance to allow evaluation for practical implementation. Specifically, there were three

objectives of this research:

1. Fabricate PES CEMs and sulfonated polyether sulfone (sPES) CEMs and characterize them.

2. Evaluate the electrodialysis performance of fabricated PES and sPES IEMs with sodium chloride solution.

3. Evaluate the selectivity features of fabricated PES and sPES membranes with real brackish water.

Chapter 2: Sulfonated PES Membranes Fabrication and Characterizations

2.1 INTRODUCTION

The importance of water scarcity to human society is growing. Besides surface water and fresh groundwater, brackish groundwater is another crucial source of water supply. However, it is necessary to remove salt from brackish groundwater or other saline water to make it drinkable. Desalination is the process of removing salinity from brackish or saline water. Electrodialysis (ED) is an electric-driven technology to remove salts among all the desalination methods. Ion exchange membranes (IEMs) are the critical components of ED technology. Thus, for the wide application of ED technology, the fabrication of cost-effective and high perm-selective IEMs is necessary and vital.

2.1.1 Recent IEMs development for ED applications

There are some IEMs fabricated for ED applications. According to the research of Zhao et al. (2019), the development of a novel cation exchange membrane was detailed. In their research, the cation exchange membrane (CEM) was fabricated using poly (p-phenylene terephthalamide) (PPTA) nanofibers and 2,5-diaminobenzenesulfonic acid (DSA) based on amide hydrolysis and amide condensation reactions. The fabrication process involves dissolving PPTA aramid nanofibers and DSA monomers in dimethyl sulfoxide (DMSO), followed by hydrolysis and condensation reactions to form the membrane. Advantages of this method include the creation of membranes with high thermal stability, resistance to organic solvents, and selective cation separation. Disadvantages may include complexity in the fabrication process and potential limitations in scalability. The ion exchange capacity leaps from 0.2 to 2.0 mmol/g, with surface electrical resistance dropping to as low as 0.71 $\Omega \cdot cm^2$, surpassing commercial alternatives. Thermally, it remains stable up to 548.5 ℃, significantly higher than commercial counterparts. In

terms of solvent resistance, after 24 hr in 80% acetone, it retains over 91% desalination efficiency. Specifically, the fabricated CEMs with PPTA/DS/PPTA materials show a salt removal rate of 95% to 99% over Na_2SO_4 and $(NH_4)_2SO_4$, after running 220 minutes, with a current density around 32 mA/cm^2. (Velocity and specific energy consumption were not reported.)

According to the research of Khan et al. (2017), the fabrication process of anion exchange membranes (AEMs) using brominated poly (2,6-dimethyl-1,4-phenylene oxide) (BPPO) and dimethylethanolamine (DMEA) was presented. The methodology involves dissolving BPPO in N-methyl-2-pyrrolidone (NMP), adding various amounts of DMEA, and casting the solution onto glass plates for solvent evaporation. The advantages of this process include producing membranes with high ion exchange capacity (1.38 mmol/g) and low area resistance (1.43 $\Omega \cdot cm^2$), beneficial for electrodialysis applications. The disadvantages might involve the complexity of the fabrication process and handling of specific chemicals like brominated compounds. This method resulted in membranes that showed a conductivity removal rate around 80% after 100 minutes. The experiment was conducted using a feed solution of 0.1 M NaCl, which flowed into the dilute cell at a constant rate of 60 mL/min. A current density of 28 mA/cm^2 was employed. And the energy consumption was 29.2 kw·h/kg.

According to the research of Gahlot et al. (2019), the synthesis and characterization of zinc metal organic framework (MOF) and sulfonated polyethersulfone (SPES) composite membranes was discussed, which focused on their electrochemical performance. The methodology involves incorporating varying amounts of Zn-MOF into the SPES matrix and assessing their physicochemical properties and performance in salt removal through electrodialysis. The “Z-2” membrane, which has 2 wt% of Zn-MOF content incorporated in SPES matrix, demonstrated superior performance with a salt removal rate of 94.1% after 200 minutes running. The experiment

was conducted with a 0.1 mol/dm^3 NaCl solution, the solution was circulated at 3 L/h, the current efficiency was 75.8%, and the specific energy consumption was 1.02 kWh/kg salt removed, the flux was 1.71 mol/m^{2}·h. The advantages include enhanced flux and lower energy consumption, while the disadvantages might relate to complexities in the fabrication process and the handling of the materials involved.

According to the research of He et al. (2016), it was described the method of preparing sulfonated poly (ether ether ketone) (SPEEK) membranes through solution casting using a mixture of ethanol and water. The process involves dissolving SPEEK in this solvent mixture, casting it onto a flat glass substrate, and drying it at various temperatures (from 80 ℃ to 160 ℃). The salt removal rate was 67.6%, with the feed solution of 0.7 mol/L NaCl, with the IEC of 2.16 meq/g, and with a current efficiency (CE) of 78.2%.

According to the research of Wu et al. (2021), a novel method for creating sub-nanoporous polyethersulfone membranes was presented. The membranes were prepared using swift heavy ion irradiation, UV sensitization, and water rinse, enabling precise control over the channel diameter at sub-nanoscale. The study used 0.1 M solutions of LiCl, NaCl, KCl, and $MgCl_2$, and a 10 V bias voltage was applied. The research demonstrated that these membranes exhibited voltage-activated ionic transport and superior selectivity in ion separation. For instance, the separation ratio of K^+: Na^+: Li^+: Mg^{2+} was as high as 83:56:14:1 for a 10-minute UV-sensitized membrane. However, the method's scalability and practicality in industrial applications needs further investigation. The membranes also demonstrated significant chemical and hydrolysis tolerance, essential for commercial use.

According to the research of Zhu et al. (2019), a novel cation-exchange membrane (CEM) enhanced with silver nanoparticles (AgNPs) using a unique in situ synthesis method was presented.

The membrane, integrating AgNPs into a sulfonated polysulfone matrix, exhibits improved mechanical, electrochemical, and antibacterial properties. In electrodialysis tests, it achieved a NaCl removal ratio of 67.5%, a high current efficiency of 96.9%, and energy consumption of 5.84 kWh/kg with a feed solution of 0.5 M NaCl. This development suggests significant potential for the membrane in antibacterial and desalting ion-exchange processes.

Gahlot et al. (2014) studied on graphene oxide nano-composite ion-exchange membranes for desalination application involved fabricating membranes using sPES and graphene oxide (GO). The salt removal was 99.1% after 118 minutes running, with a feed solution of 0.1 M NaCl, and the CE was 97.4%, the IEC was 1.27 meq/g, the constant applied potential was 2.0 V per cell pair.

Fan et al. (2023) investigated the development and characterization of asymmetric cation exchange membranes optimized for ED desalination. Using a novel approach, sPES was incorporated into porous PES substrates to create a thin, selective layer with enhanced hydrophilicity and porosity. This design significantly improved ion transport and dimensional stability, even at low ion exchange capacities, leading to superior ED performance. In the ED tests, NaCl solution with a conductivity of 11 mS/cm (equivalent to 0.1 mol/L NaCl) was used as feed solution, after 120 minutes running, the prepared 40%sPES-PES membrane (with an IEC of 0.52 mmol/g) exhibited a salinity reduction rate of 91.9%, a current efficiency of 127.5%, and low energy consumption of 5.55 kw·h/kg.

Zhao et al. (2020) explored the fabrication of cation exchange membranes using sPES and polyvinylpyrrolidone (PVP) to enhance ED performance. Through innovative material combination and structural design, the research aimed to optimize membrane properties for improved stability, ion transport, and desalination efficiency. In the detailed ED performance, 50 g/L NaCl (equivalent to 0.86 mol/L NaCl) was used as feed water. The fabricated

sPES/PVP K30 membranes with an IEC of 0.54 mmol/g showed a salinity reduction of 90% after 200 minutes running, and the corresponding current density was 14 mA/cm^2, the current efficiency was 80%, and the energy consumption was 11.6 kW·h/L.

Mabrouk et al. (2021) made a new ion exchange membrane for ED desalination of brackish water, named ClNH2, from sulfochlorated PES (Cl-PES), and crosslinked with aminated PES (NH2-PES). The ClNH2 membrane had an ion exchange capacity of 2.2 meq/g. In the ED experiments, the feed solution was 3 g/L NaCl solution, and the flow rate was 10 L/h, the applied voltage was 1 V/cell-pair. After 15 minutes running, the salinity reduction was 93.8%, and the specific power consumption was 2.5 W·h/L.

More comparisons are shown in Table 2.1. As shown in Table 2.1, although there have been many IEMs developed by researchers for ED applications, most of them were fabricated with complicated physical or chemical treatment or crosslinked with some other materials, making the fabrication process quite complicated or not cost-effective. The goal of this work is to evaluate the use of simple polyether sulfone (PES) and sulfonated PES (sPES) alone (without complicated additives or mixtures) for the fabrication of IEMs for ED application.

Table 2.1 Summary of IEMs developed for ED applications.

Sample	Membrane Material	IEC (meq/g)	CE (%)	Salt Removal (%)	Feed Solution (mol/L)	Reference
PDP-2.0	PPTA/DS/PPTA	1.6	-	95.1	0.08 Na_2SO_4	(Y. Zhao, Qiu, et al., 2019)
S/P/PANi-0.6	SPES/PVP/PANi	0.47	94.3	-	0.1 NaCl	(J. Zhao et al., 2019)
PAN-PAMPS-2	PAN/PAMPS	1.65	91	-	0.35 NaCl	(Pal et al., 2019)
DES-5	SPES/S-MoS2	1.42	69.5	-	0.1 NaCl	(J. Zhu, Liao, et al., 2019)
60SPSF-C2	SPSF/Acrylic crosslinker	1.6	95.7	91.7	0.1 NaCl	(Khan et al., 2017)
PVA/BFC-70	PVA/DVB/AMPS	1.3	87.5	-	0.85 NaCl	(Thakur et al., 2015)
SPI/PGO-8	SPI/PGO	2.37	76.4	-	0.1 NaCl	(Shukla et al., 2016)
SPK/IGO-8	SPEEK/IGO	2.23	82.9	-	0.85 NaCl	(Chen et al., 2020)
SPSU-60	SPSF/AgNP	1.55	96.9	67.5	0.5 NaCl	(J. Zhu, Luo, et al., 2019)
Z-2	Zn-MOF/sPES	-	75.8	94.1	0.1 NaCl	(Gahlot et al., 2019)
SG-10	SPES/GO	1.27	97.4	99.1	0.1 NaCl	(Gahlot et al., 2014)
SGO-5	SPES/SGO	1.7	93.1	-	0.1 NaCl	(J. Zhao et al., 2018)
S-25/P	SPES/PVP	0.65	-	-	0.1 NaCl	(P. P. Sharma et al., 2018)
SPEEK/PGO-8	SPPEK/PGO	2.16	78.2	67.6	0.7 NaCl	(He et al., 2016)
70% S-PVDF	SPVDF/PVDF	0.7	-	-	0.1 NaCl	(P. P. Sharma et al., 2017)
MIL-10	SPES/MIL-101	1.04	85	-	0.1 NaCl	(P. Sharma & Shahi, 2020)
PM-5	PVC/St/DVB/SGO	1.76	82.3	-	0.085 NaCl	(P. P. Sharma et al., 2016)
CEM-3	PAN/PStSO_3Na/PnBA	1.47	76.8	-	0.085 NaCl	(Pismenskaya et al., 2018)
40%sPES-PES	sPES/PES/PVP	0.52	127.5	91.9	0.1 NaCl	(Fan et al., 2023)
Sub-nanoporous PES	PES	-	-	-	0.1 LiCl, NaCl, KCl, $MgCl_2$	(Wu et al., 2021)
S/P K30	sPES/PVP	0.54	80	90	0.86 NaCl	(J. Zhao et al., 2020)
ClNH2	Cl-PES/NH2-PES	2.2	-	93.8	0.05 NaCl	(Mabrouk et al., 2021)

2.2 MATERIALS AND METHODOLOGY

2.2.1 Materials

Polyether sulfone (PES) was purchased from Goodfellow (SU30-GL-000111, norminal granule size 3 mm, molecular weight 58,000 g/mol, melt volume rate: 35 (360 ℃/10 kg), cc/10 min, USA). Dichloromethane (DCM, CH_2Cl_2) (ACS grade, BDH, USA) was used as the solvent for PES during the sulfonation process. Chlorosulfonic acid (CSA, HSO_3Cl) (>98.0%, Fluka, USA) was used as the sulfonating agent, and N-Methyl-2-pyrrolidone (NMP, C_5H_9NO) (ACS grade, Fisher Scientific, USA) was used for the solvent purification in membrane fabrication. Petri dishes were used to cast the membranes.

Laboratory-grade (ACD reagent grade) sodium chloride (NaCl) and sodium sulfate (Na_2SO_4) were purchased from Fisher Scientific (USA) to prepare the feed solutions and the electrode rinse solution, respectively. All the ED tests (except LCD tests) were performed in triplicate.

2.2.2 Fabrication of PES and sPES Membranes

2.2.2.1 Fabrication of PES membranes

The fabrication diagram of PES cation exchange membranes was shown in Figure 2.1. Firstly, 30 g of PES pellets were weighed and dissolved into 170 g NMP solvent, making 200 g PES dope solution for subsequent use. Secondly, 2.0 g PES dope solution was cast into each Petri dish and left at room temperature to evaporate for 0.5 hr, 1 hr, 2 hr, 3 hr, 4 hr, 8 hr,16 hr, and 24 hr, respectively. Then, those Petri dishes were submerged in DI water to form the PES membranes

through the phase inversion effect.

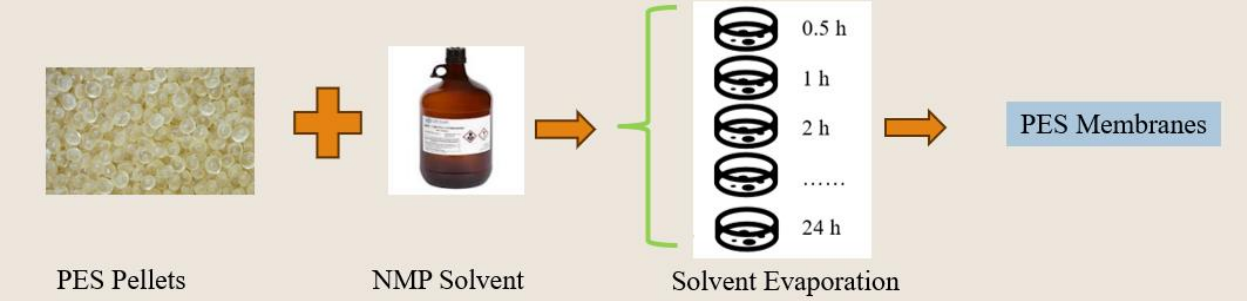

Figure 2.1: PES membranes fabrication diagram.

Examples of selected cast PES membranes with 1 hr, 4 hr, 8 hr, and 24 hr solvent evaporation times are shown in Figure 2.2. As shown in the figure, the PES membrane with 1 hr solvent evaporation time has no transparency. With the increase of solvent evaporation time, the PES becomes more transparent. When the time reaches 24 hr, the PES becomes transparent.

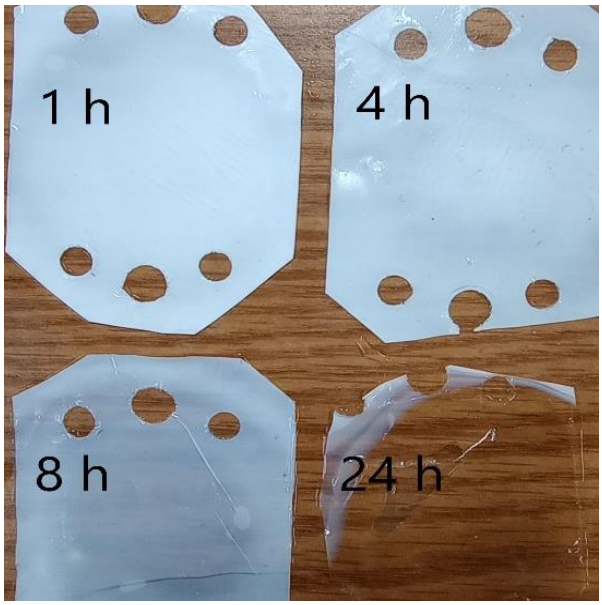

Figure 2.2: PES membrane examples with 1 hr, 4 hr, 8 hr, and 24 hr solvent evaporation time.

2.2.2.2 Fabrication of sPES membranes

The general fabrication diagram of sPES cation exchange membranes is shown in Figure 2.3. The first step is sulfonation by CSA (Cao et al., 2010; KIM et al., 1999; Tavangar et al., 2020; Unnikrishnan et al., 2010). As shown in Figure 2.4, the sulfonation process would increase the content of the HO_3S^- group. Specifically, blank PES (bPES) weighed 30 g and was

dissolved into 150 mL DCM. Then, 8 mL CSA was added, and the mixture was stirred for 60 min. The mixture was quenched with 300 mL methanol. The phase inversion method was applied to solidify sulfonated PES (sPES) by adding 170 g NMP to form sPES solution and slowly pouring sPES/NMP solution into DI to form sPES noodles. The noodles soaked for over 24 hr to neutralize pH. The process was repeated three times to thoroughly neutralize pH. The solid sPES material was removed and placed under the fume hood to fully dry for subsequent use. In addition to 8 mL CSA, different sulfonation degree was tried with 16 mL and 24 mL CSA. However, the sPES cannot form a membrane with 24 mL CSA after purification. Also, with 16 mL CSA, the formed sPES membranes were fragile in mechanical strength, which means they were fragile and easily broken. Thus, the sulfonation method with 8 mL CSA was chosen for the following experiments.

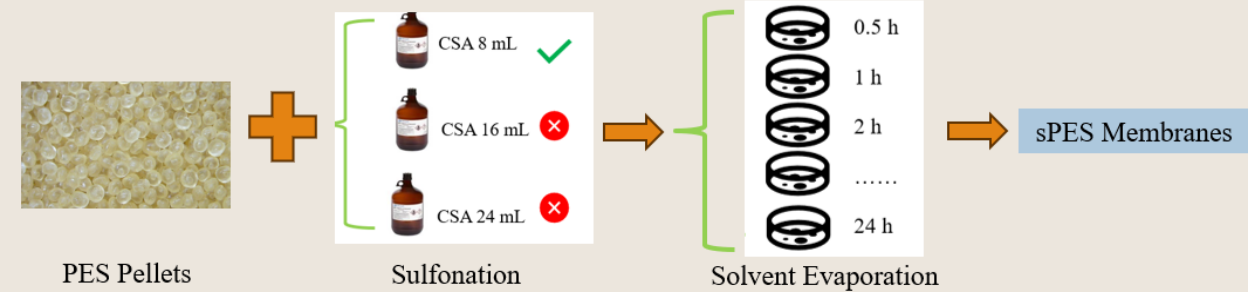

Figure 2.3: sPES membranes fabrication diagram.

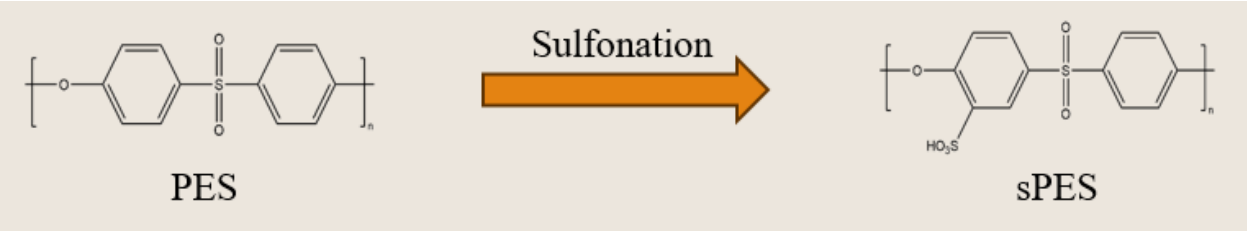

Figure 2.4: Molecular formula of PES and sPES polymers.

After the dry sPES material was produced, the second step was like the fabrication process of PES membranes. The sPES dope solution was made for the membrane's fabrication process. Firstly, 30 g sPES was weighed and put into 170 g NMP to make a 15% sPES dope solution. Secondly, 2.0 g sPES dope solution was cast into each petri dish and put in the air to evaporate for

0.5 hr, 1 hr, 4 hr, 8 hr, 12 hr, 16 hr, 20 hr, and 24 hr, respectively, then they were submerged in DI water to form the sPES membranes.

Examples of selected cast sPES membranes with 0.5 hr, 8 hr, 16 hr, and 24 hr solvent evaporation times are shown in Figure 2.5. From the figure, 0.5 hr sPES has no transparency. With the increased solvent evaporation time, the sPES membranes become gradually transparent. When the time reaches 24 hr, the sPES membranes become transparent.

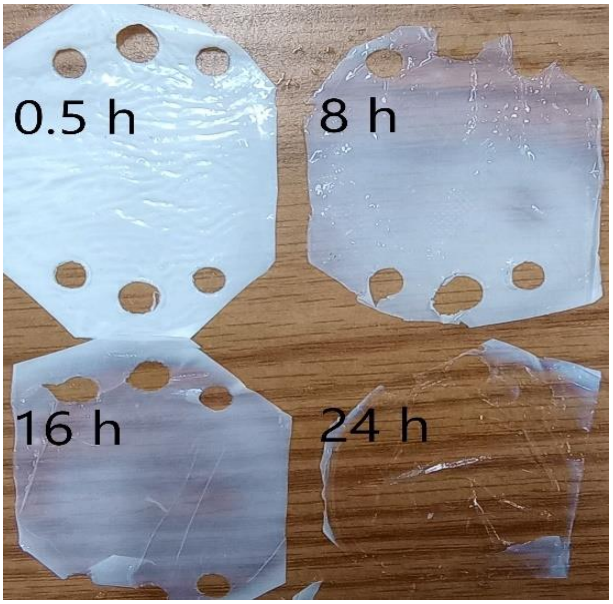

Figure 2.5: sPES membrane examples with 0.5 hr, 8 hr, 16 hr, and 24 hr solvent evaporation time.

2.2.3 Membrane Characterization Methods

2.2.3.1 Degree of sulfonation (DS) measurements

The degree of sulfonation (DS) is the fraction of the sulfonated monomer units after the reaction. Membranes were dried and weighed, then soaked in 2 M NaCl solution for 24 hr to release the sulfonic acid groups into the solution. Next, sodium hydroxide with a concentration of 0.1 M was titrated into the mixture. Phenolphthalein was used as an indicator. The following formula was used for the calculation of DS (Guan et al., 2005; Klaysom, Ladewig, et al., 2011; Z.

Li et al., 2018):

$$DS = \frac{244\ {}^{g}/_{mol}\,(C_{NaOH} \times V_{NaOH})}{W - 81\ {}^{g}/_{mol}\,(C_{NaOH} \times V_{NaOH})} \quad (2.1)$$

Where C_{NaOH}, V_{NaOH}, and W are the concentration (mol/L) of standard NaOH solution, volume (mL) of NaOH solution used for neutralization, and weight (g) of dry IEMs, respectively. The molecular weight of the PES repeating unit is 244 g/mol, and 81 g/mol is the molar mass of the sulfonate SO_3H group.

2.2.3.2 Ion-exchange capacity (IEC) measurements

Ion-exchange capacity (IEC) measures a material's capability to exchange ions formerly incorporated within its structure. Specifically, the membranes were soaked for 24 hr in 1 M HCl and rinsed with deionized water to remove the acid from the surface. Then, immerse the membranes in 2 M NaCl for 24 hr. Then, the solution was titrated with NaOH using phenolphthalein as an indicator. The IEC (meq/g) was calculated using the following formula (Klaysom, Moon, et al., 2011; Z. Li et al., 2018):

$$IEC = \frac{C_{NaOH} \times V_{NaOH}}{W_{Dry}} \quad (2.2)$$

Where, C_{NaOH}, V_{NaOH}, and W_{Dry} are the concentration (mol/L) of standard NaOH solution, volume (mL) of NaOH solution used for neutralization, and weight (g) of dry IEMs.

2.2.3.3 Fourier transform infrared-attenuated total reflectance (FTIR-ATR) measurements

Fourier transform infrared (FTIR-ATR) analysis was conducted using a Nicolete™ iS™ 5 FTIR equipped with an iD7 attenuated total reflectance (ATR) Diamond (Thermo Fisher Scientific, Waltham, MS, USA). All FTIR-ATR data sets were normalized by dividing the signal output by the intensity of the highest peak in the series. Technically, there is a difference between FTIR and FTIR-ATR methods; the major difference is that in FTIR, the material observation is generated by

the infrared radiation passing through a sample, and some is absorbed, whereas, FTIR-ATR is based on the principle that molecules absorb specific frequencies of infrared (IR) light, corresponding to the vibrational energies of their chemical bonds. Each type of bond has a characteristic absorption frequency, and the pattern of these frequencies can be used to identify functional groups and molecular structures. In ATR, an IR beam is directed onto an optically dense crystal with a high refractive index. The IR light reflects internally in the crystal, and, at each reflection, a small amount of energy penetrates into the sample placed on the crystal's surface. This penetration, typically only a few micrometers deep, allows the IR light to interact with the sample. The ATR technique simplifies sample preparation, as it can analyze samples in various states (solid, liquid, or gas) without extensive preparation. It is particularly useful for analyzing thick or non-transparent samples that would be difficult to analyze using traditional transmission IR spectroscopy. In this research, FTIR-ATR was used to characterize the molecular functional groups in the IEMs.

2.2.3.4 Atomic force microscopy (AFM) measurements

AFM was utilized for material characterization analyses primarily due to its capability to provide high-resolution imaging at the atomic or molecular level. This is essential for understanding the surface structure and properties of materials. One of the key advantages of AFM is its non-destructive nature, meaning it does not alter or damage the sample under study, which is crucial for delicate or expensive materials. Additionally, AFM is versatile, capable of operating in various conditions - air, vacuum, or liquid, and is suitable for a diverse range of materials, including biological specimens, polymers, and nanomaterials. AFM not only allows for analysis of surface topography but also can assess mechanical, electrical, and magnetic properties of the material. The technique involves minimal sample preparation compared to other high-resolution

methods. In terms of its working principle, AFM operates by scanning a sharp tip, mounted on a cantilever, over the sample surface. The interaction forces between the tip and the sample cause the cantilever to deflect, which is detected by a laser and photodetector system. This system employs a feedback loop to maintain constant force, preventing damage to the tip or sample. The data from the photodetector is processed to generate a detailed map of the surface topography and properties.

The AFM in this research was performed using a standard commercial tip (Bruker DNP- S10) with a spring constant of 0.12 N/m. All the AFM images were acquired in ambient air using tapping mode and digitized into 512 pixels x 512 pixels. A variety of scans were performed at random localities on the film surface to analyze the AFM images and the topographic image data were converted into ASCII data for analysis.

2.2.3.5 X-ray photoelectron spectroscopy (XPS) measurements

XPS (Thermo Nexsa g2) was used for material characterization analysis, primarily for its ability to provide detailed information about the elemental composition, chemical states, and electronic states of materials at the surface level. This surface sensitivity, typically up to 10 nm deep, makes XPS invaluable for studying thin films, coatings, surface treatments, and interfaces in a range of materials. The technique operates by irradiating a material with a beam of X-rays, which causes the emission of photoelectrons from the surface atoms. The kinetic energy of these emitted photoelectrons is measured and used to determine the binding energies of the electrons, which are unique to specific elements and their chemical states. By analyzing these energy levels, XPS can be used to identify the elements present, their quantities, and chemical bonding states, providing a comprehensive surface chemical analysis.

2.3 RESULTS AND DISCUSSION

2.3.1 Preliminary Results

Based on different solvent evaporation times, 0.5 hr, 1 hr, 2 hr, 3 hr, 4 hr, 8 hr, 16 hr, and 24 hr, different PES membranes were fabricated. Preliminary results were generated to optimize the fabrication based on preliminary running conditions, like 3 g/L NaCl feed solution, 3 cm/s flow velocity, and 0.8 v/cell-pair. As shown in Figure 2.6 (a), with solvent evaporation times from 0 to 3 hr, the current density increases, which means the membrane resistance decreases. When the solvent evaporation time is 3 hr, the current density of PES shows the best performance, which is 97 A/m^2. Furthermore, when the solvent evaporation time increases beyond 3 hr, the current density decreases. After 8 hr evaporation time, the current density decreased to 10 A/m^2. It is probably because the evaporation of solvent decreases the resistance. After 3 hr, the current density decreases, increasing the membrane resistance. It is probably because of the membrane becoming denser, the porosity becoming small, and even no porosity stopping ions from passing through.

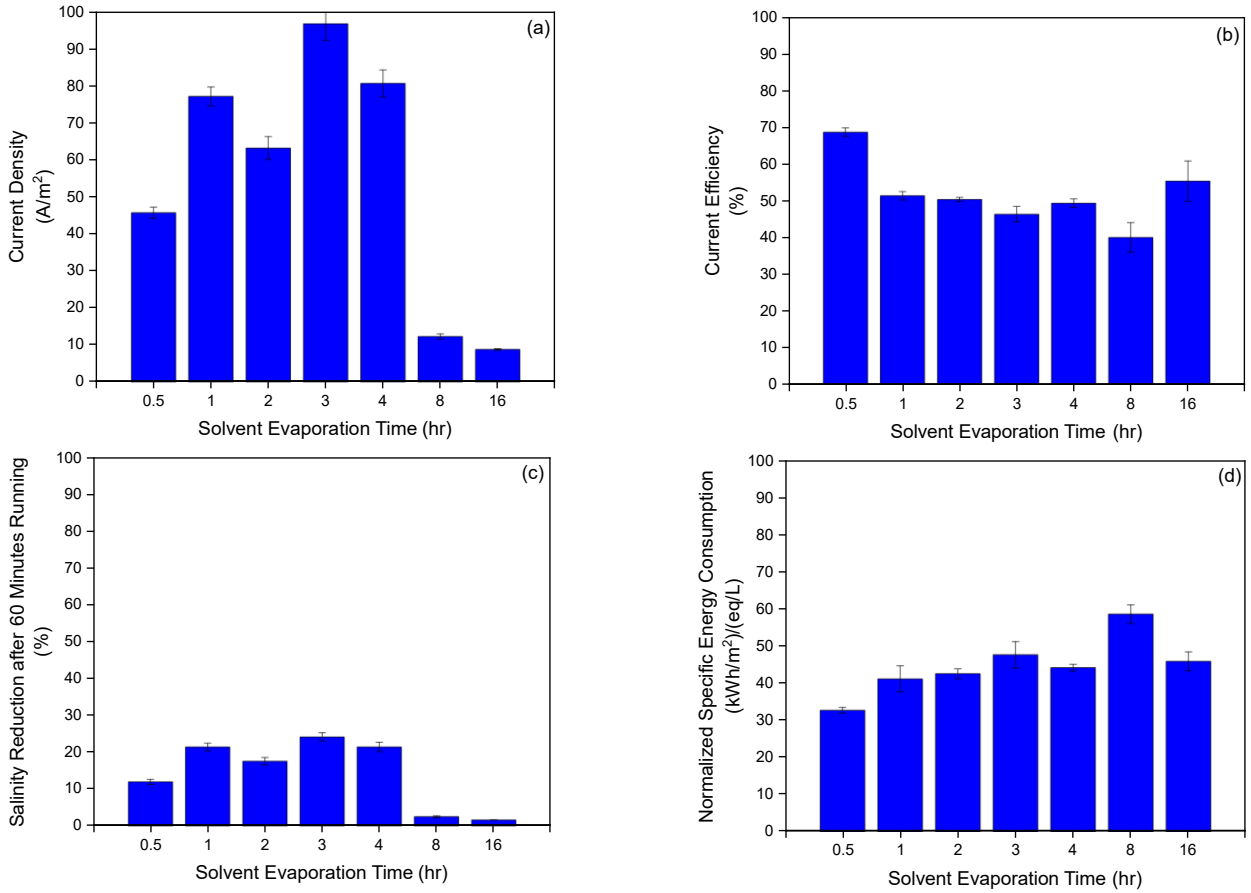

Figure 2.6: Preliminary ED performance results of PES membranes in different solvent evaporation times: (a) current density (CD), (b) current efficiency (CE), (c) salinity reduction (SR) after 60 minutes running, and (d) normalized specific energy consumption (nSEC).

As shown in Figure 2.6 (b), when the solvent evaporation time is 0.5 hr, the current efficiency of PES shows the best performance, 69%. However, most of the PES membranes show a current efficiency of 50%, meaning that 50% of the electricity was used to remove salts. As shown in Figure 2.6 (c), the best performance of salinity reduction after 60 minutes occurred when the PES solvent evaporation time is 3 hr (24% removal). Starting from 8 hr solvent evaporation time, the salinity reduction performance decreases substantially. As shown in Figure 2.6 (d), most

PES membranes show a normalized specific energy consumption range of 40-50 kWh/m^3/(eq/L).

Based on different solvent evaporation times (0.5 hr, 1 hr, 4 hr, 8 hr, 12h, 16 hr, 20 hr, and 24 hr), different sPES membranes were fabricated. Moreover, preliminary results were generated to optimize the fabrication based on preliminary running conditions, like 3 g/L NaCl feed solution, 3 cm/s flow velocity, and 0.8 v/cell-pair. As shown in Figure 2.7 (a), when the solvent evaporation time is within 1 hr, the current density of sPES shows the best performance, which is 130 A/m^2. Moreover, when the solvent evaporation time increases, the current density decreases gradually. Starting from 24 hr, the current density decreases obviously, and the lowest is 10 A/m^2 when the solvent evaporation time is 24 hr. From 20 hr, the current density decreases obviously, which means the membrane resistance increases obviously. It is probably because of the membrane becoming denser, the porosity becoming small, and no porosity stopping ions from passing through. Compared with the current density of PES membranes, the changes of current density of sPES membranes are much smaller; this indicates that the sulfonation process greatly decreases the influence of solvent evaporation.

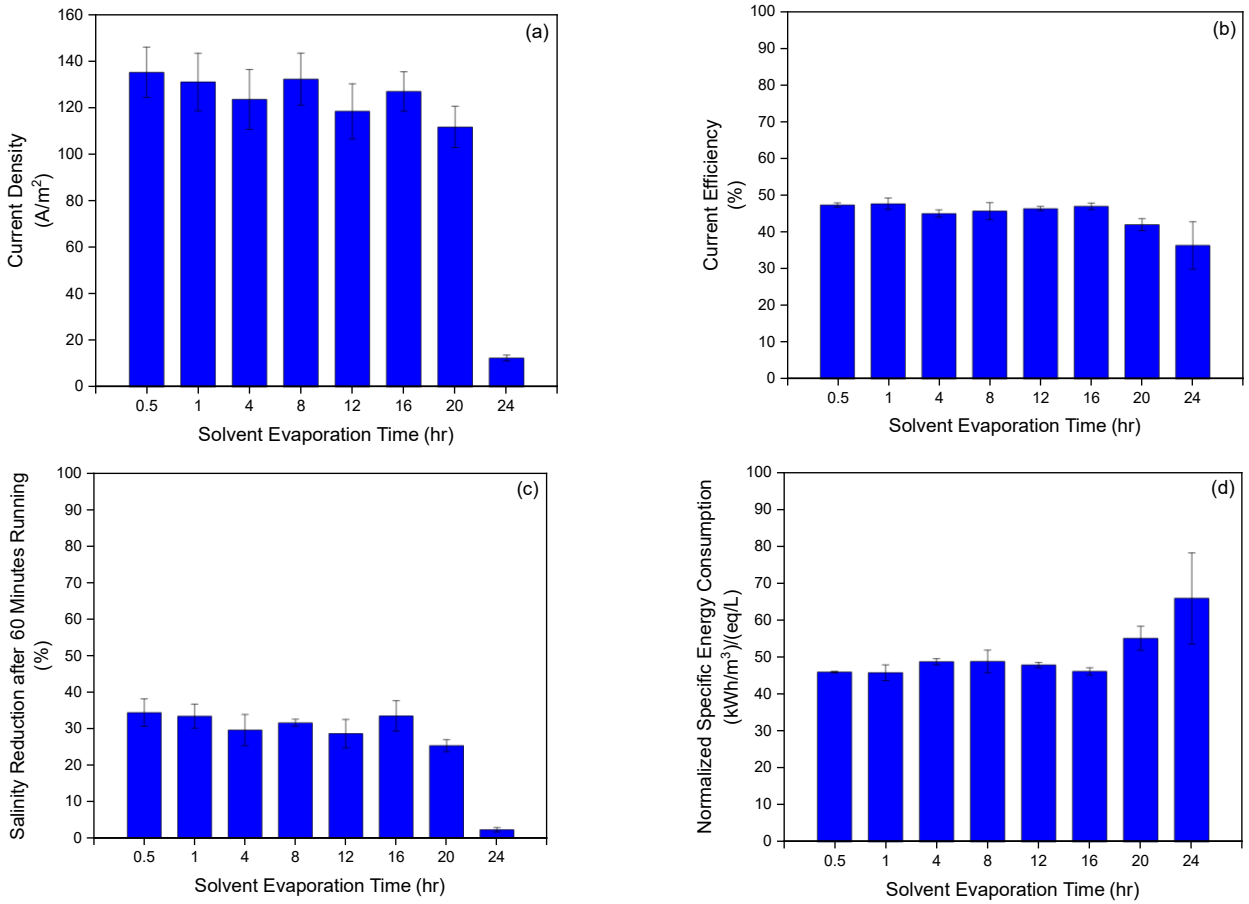

Figure 2.7: Preliminary ED performance results of sPES membranes in different solvent evaporation times: (a) current density (CD), (b) current efficiency (CE), (c) salinity reduction (SR) after 60 minutes running, and (d) normalized specific energy consumption (nSEC).

As shown in Figure 2.7 (b), most of the sPES membranes show a current efficiency of 48%, which means that 48% of the electricity was used to remove salts. In addition, starting from 24 hr solvation evaporation time, the current efficiency performance decreases substantially. Compared with the PES membranes, while the current density of the sPES membranes is higher, the current efficiency of sPES membranes is slightly lower than that of the PES membranes. These results may indicate that the higher current density doesn't have effects on current efficiency. With more ions passing through sPES membranes, there may be more co-ions passing through sPES membranes too, which resulted in slightly lower current efficiency. As shown in Figure 2.7 (c)

when the solvent evaporation time is within 1 hr, the salinity reduction after 60 minutes of running sPES membranes shows the best performance, which is 33%. Starting from 20 hr, the salinity reduction performance decreases substantially. As shown in Figure 2.7 (d), when the solvent evaporation time is within 1 hr, the normalized specific energy consumption of sPES shows the best performance, which is 45 $kWh/m^3/(eq/L)$. Moreover, starting from 20 hr, the normalized specific energy consumption performance increases substantially.

Based on the results shown in Figure 2.6, it can be concluded that for PES membranes, when the solvent evaporation time is 3 hr, the general performance of PES membrane is the best. For sPES membranes, as shown in Figure 2.7, when the solvent evaporation time is within 1 hr, the general performance of the sPES membrane is the best. Therefore, PES membranes and sPES membranes with the best performance were chosen for the future analysis, which means PES membranes with a solvent evaporation time of 3 hr and sPES membranes with a solvent evaporation time of 1 hr were selected for subsequent studies.

2.3.2 Membrane characterization results

As shown in Table 2.2, according to Equation 2.1 and Equation 2.2, the ion exchange capacity of the best PES membrane is 1.5 meq/g, and the corresponding sulfonation degree is 42%. The ion exchange capacity of the best sPES membrane is 2.67 meq/g, and the corresponding sulfonation degree is 83%.

Table 2.2: Ion exchange capacity and sulfonation degree of selected PES and sPES membranes.

	IEC (meq/g)	**SD (%)**
PES	1.5	42
sPES	2.67	83

As shown in Figure 2.9, the FTIR-ATR figure of PES and sPES membranes were presented. The absorption peak at 1010 cm^{-1} is characteristic of the aromatic SO_3H symmetric stretching vibrations (Noel Jacob et al., 2014). Furthermore, the normalized intensity of sPES is slightly

stronger than PES. We can conclude that sulfonic acid groups have been introduced into the polymer chains.

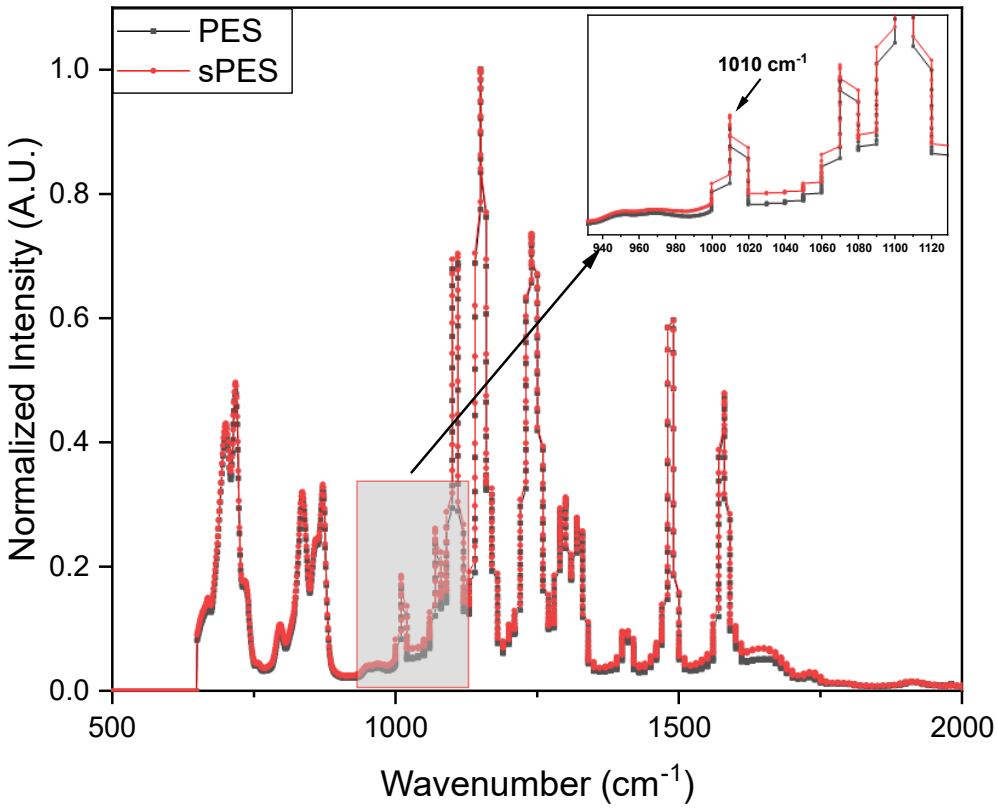

Figure 2.8: FTIR-ATR figure of selected PES and sPES membranes.

As shown in Figure 2.9, the XPS figure of PES and sPES membranes were presented. The peak at 168 eV is characteristic of S2p, which indicates the existence of SO_3H (Fan et al., 2023). From the XPS figure, the sulfonic acid group of sPES is slightly stronger than PES, which can be resulted from the sulfonation process of sPES membranes.

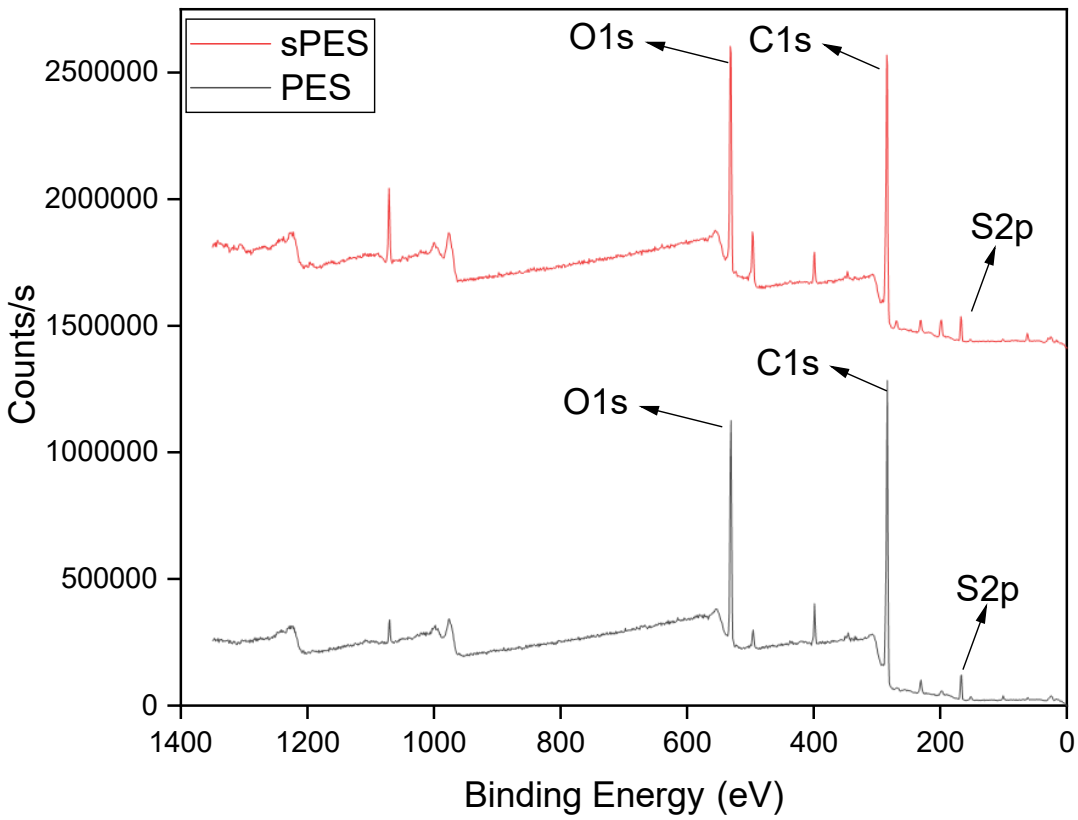

Figure 2.9: XPS figure of selected PES and sPES membranes.

The surface morphologies of the PES and sPES characterized by AFM are shown in Figure 2.10. Surface changes reflect the influence that sulfonation has on the membrane morphology and can be observed by difference in the mean roughness (Ra). Consistent with previous research findings, the Ra parameters increased from PES (0.996 nm) to sPES (3.149 nm) from with an increase in the sulfonation in the casting solution (Rahimpour et al., 2010). For PES, a relatively flatter smooth-phase morphology can observed, but the sPES has more cluster-like features clearly seen in 1µm x 1µm analyses, likely due to an increase in degree of sulfonation (Guan et al., 2005).

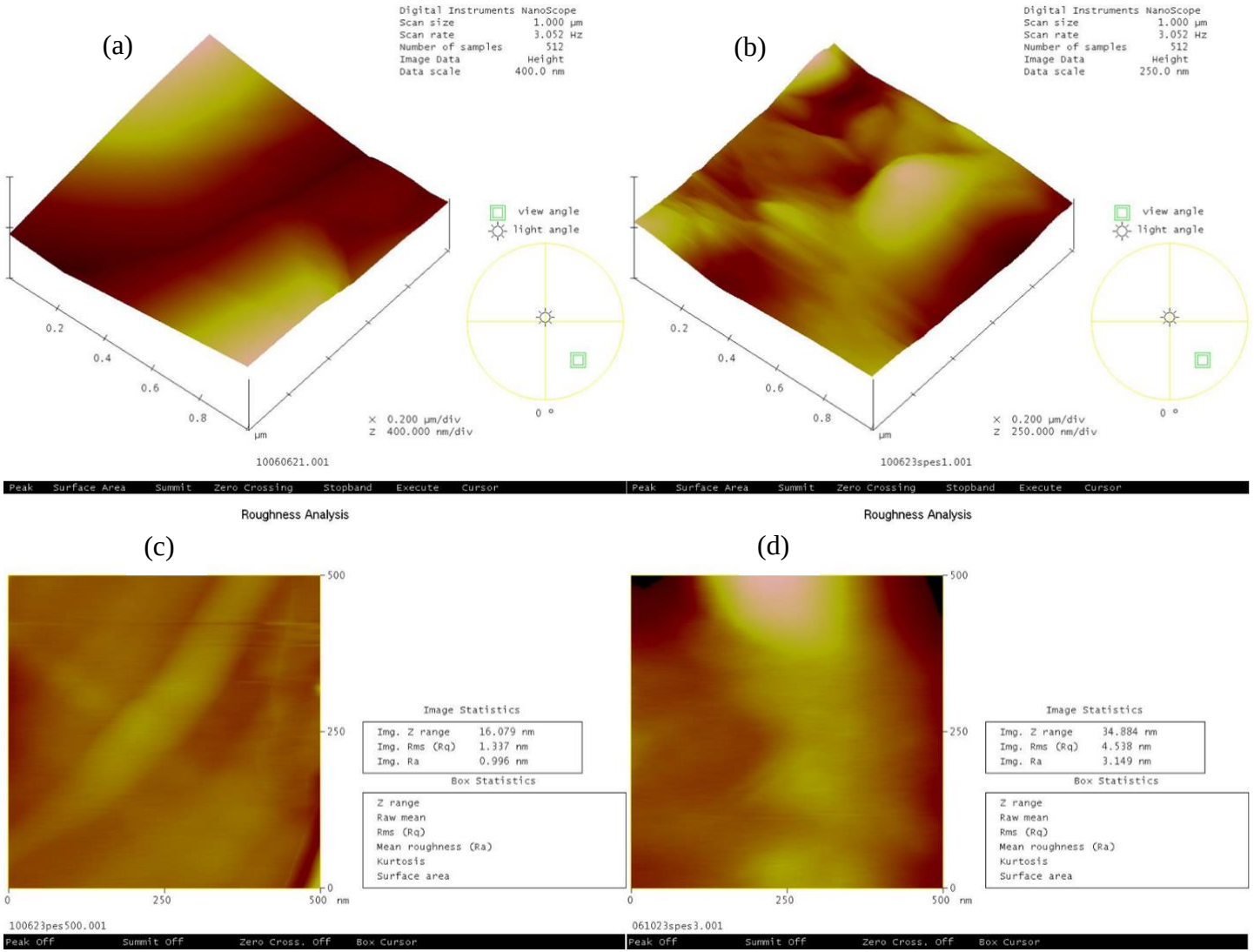

Figure 2.10: AFM figures of selected PES and sPES membranes: 1µm x 1µm AFM images of (a) PES and (b) sPES; 0.5µm x 0.5µm surface roughness analysis of (c) PES and (d) sPES.

2.4 CONCLUSION

The study of fabricated PES and sPES IEMs and their characterization analysis results are summarized below. Based on electrodialysis testing with PES membranes with different solvent evaporation times, the solvent evaporation time of 3 hr was determined to be optimal based on several figures of merit (*e.g.*, current density, current efficiency, salinity reduction, and normalized specific energy consumption), while the sPES membranes evaporated within 1 hr show the best performance based on the same figures of merit. With electrodialysis test conditions of 3 cm/s flow velocity, 0.8 V/cell-pair, and 3 g/L NaCl feed water, for PES membranes, the average current density was 97 A/m^2, the current efficiency was 50%, the salinity reduction after 60 minutes of running was 24%, and the normalized specific energy consumption was approximately 45 $kWh/m^3/(eq/L)$. Under the same running conditions, for sPES membranes, the average current density was 130 A/m^2, the current efficiency was 48%, the salinity reduction after 60 minutes of running was 33%, and the normalized specific energy consumption was approximately 45 $kWh/m^3/(eq/L)$. ED performance shows that the process of sulfonation increases the general salinity reduction from PES membranes to sPES membranes.

The increase of surface roughness from PES membrane (0.996 nm) to sPES (3.149 nm) membrane from AFM images, and the strengthened FTIR-ATR and XPS figure of sPES show the effect of sulfonation process which increases the degree of sulfonation.

Chapter 3: PES and sPES Cation Exchange Membranes Electrodialysis Performance Evaluation with Sodium Chloride Solution

3.1 INTRODUCTION

Based on the fabricated IEMs in the previous chapter, further evaluation of the ED performance was analyzed by treating a 3 g/L NaCl solution. Neosepta commercial membranes were used as a comparison. Finally, basic materials cost was estimated for reference.

3.2 METHODOLOGY

3.2.1 Electrodialysis Test Method:

NaCl solution with a concentration of 3 g/L was prepared. A PCCell Micro ED (7.48 cm^2) was used to assemble a stack with cation and anion exchange membranes alternated, and in between membranes were spacers. Each stack was assembled with five cell pairs.

LabVIEW SCADA software system collected test data (electrical current, stack voltage, and conductivity of process streams). ED tests were designed with different stack voltages (0.4 and 0.8 V/cell-pair) and flow velocities (3 and 6 cm/s). ED tests were started with equal volumes of diluate and concentrate, which represented a nominal hydraulic recovery of 50%. Sodium sulfate (Na_2SO_4) solution with a concentration of 14.2 g/L was used as an electrode rinse solution. Commercially available Neosepta AMX76 and CMX76 ion exchange membranes were used to compare to the novel PES and sPES membranes. The ED tests were performed for 60 minutes, each in triplicate (except LCD tests). The detailed experimental variables and value ranges are shown in Table 3.1 (Hyder et al., 2021).

Table 3.1: Experimental variables and value ranges.

Variables	Values
Feed Water	3 g/L NaCl solution
Flow Velocity	3, 6 cm/s

Stack Voltage	0.4, 0.8 voltage per cell-pair
Combination of Membranes	i) PES & Neosepta AMX76 ii) sPES & Neosepta AMX76 iii) Neosepta CMX76 & AMX76

3.2.2 Calculation Methods:

3.2.2.1 Current Density

Electrical current density is the amount of electrical current passing through the membranes' active area inside the electrodialysis stack. The current density (i) was calculated using the following formula (Walker et al., 2014):

$$i = \frac{I}{A} \tag{3.1}$$

Where, I is the electric current (A), A is the membrane active transfer area (7.48 cm^2 for the PCCell MicroED).

3.2.2.2 Limiting Current Density (LCD)

The limiting current density (LCD) is the maximum allowable current density at which the concentration of salt ions at the membrane surface becomes zero at the membrane surface inside the diluate cell of the electrodialysis stack. The electrodialysis system should operate at a current density less than LCD to prevent water splitting, power wastage, and equipment damage. An example figure of LCD is shown in Figure 3.1, which shows the limiting current region. (Káňavová et al., 2014; Krol et al., 1999; Lee et al., 2006; Strathmann et al., 1997) .

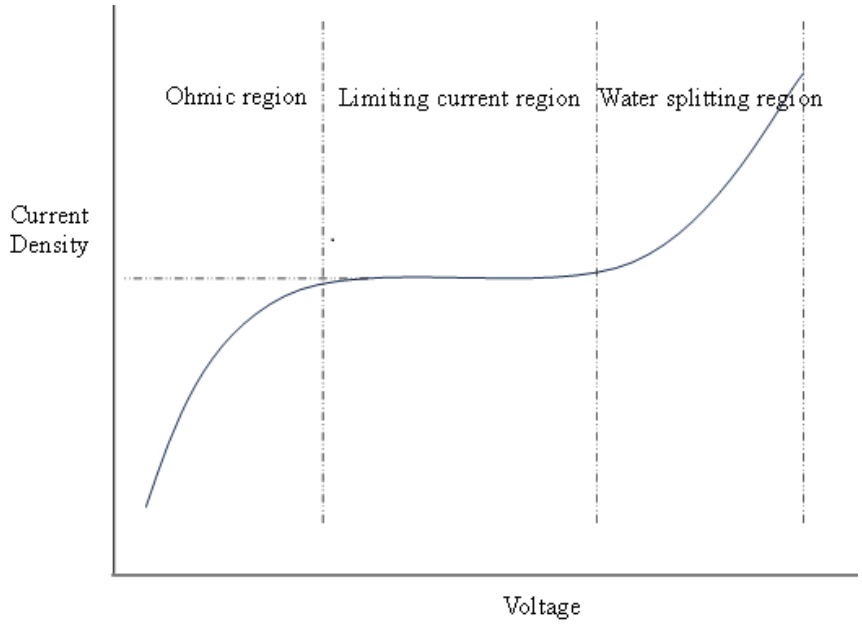

Figure 3.1: Typical current-voltage curve within ohmic region, limiting current region, and water splitting region [adapted from (Káňavová et al., 2014)].

3.2.2.3 Current Efficiency

Current efficiency is also known as the current utilization, which is the ratio between the amount of the current used in the electrodialysis stack to effectively separate salt ions and the amount of the total current applied to the stack. Current efficiency (ξ) was calculated using the formula below (Campione, 2018; Sadrzadeh & Mohammadi, 2009; Strathmann, 2010):

$$\xi = \frac{(C_f - C_d)QF}{IN_{cp}} \tag{3.2}$$

Where, C_f and C_d are the concentrations (mol/L) of feed solution and diluate solution, respectively. Q is the diluate and concentrate flow rate (L/s), F is the Faraday constant (96485 Coulombs/eq or Amp-s/eq), I is the measured electrodialysis stack current (Amp), and N_{cp} is the number of cell-pair in electrodialysis stack.

3.2.2.4 Salinity Reduction

Salinity reduction is the ratio of salt concentration reduction from the initial salt

concentration in the diluate stream as a function of experimental time. The salinity reduction (SR) was calculated using the formula below (Walker et al., 2014):

$$R = \frac{(C_f - C_d)}{C_f} \tag{3.3}$$

Where, C_f and C_d are the concentrations (g/L) of feed solution at the beginning of the experiment and diluate solution at any time (t = 60 minutes in this study) of the experiment. The concentration of sodium chloride was calculated from measured electrical conductivity by the following equation:

$$C = 1.224 \times 10^{-9}\kappa^4 - 3.243 \times 10^{-7}\kappa^3 + 5.135 \times 10^{-5}\kappa^2 + 8.869 \times 10^{-5}\kappa \tag{3.4}$$

Where, κ is the electrical conductivity in units of mS/cm. This equation is an empirical fit of CRC data (Vanysek, 2012) and Landolt-Börnstein data (Landolt-Börnstein, 1960).

3.2.2.5 Normalized Specific Energy Consumption (nSEC)

Normalized specific energy consumption (nSEC) [expressed as (kWh/m^3) per (meq/L)] was the amount of energy consumption required to produce one cubic meter of product water per mmol/L of salt removal.

The DC electrical power ($P_{electrical}$) consumed by the electrodialysis stack was calculated using the formula as follow (Walker et al., 2014):

$$P_{electrical} = \Delta V_{stack} I \tag{3.5}$$

Where, ΔV_{stack} is the voltage drop across the electrodialysis stack (V), and I is the electrical current measured through the electrodialysis stack (A).

The hydraulic power ($P_{hydraulic}$) for pumping the solution through the electrodialysis stack was calculated using the formula as below (Walker et al., 2014):

$$P_{hydraulic} = \rho g Q \Delta H \tag{3.6}$$

Where, ρ is the solution mass density, g is the gravitational constant, Q is the volumetric

flow rate, and ΔH is the hydraulic head loss through the stack.

The specific energy consumption (SEC) was calculated using the formula below (Walker et al., 2014):

$$SEC = \frac{P_{electrical} + P_{hydraulic}}{Q_d} \tag{3.7}$$

Where, P is the power (kW) and Q_d is the flow rate of the diluate stream (m^3/h).

Normalized SEC was calculated using the formula below (Walker et al., 2014):

$$SEC_{normalized} = \frac{SEC}{C_f - C_d} \tag{3.8}$$

Where, C_f is the concentration of feed solution at the beginning of the experiment (meq/L) and C_d is the concentration (meq/L) of diluate solution at any time (t) of the experiment.

3.3 RESULTS AND DISCUSSION

3.3.1 Limiting Current Density (LCD)

The current density of Neosepta, PES and sPES membranes is shown in Figure 3.2 for treating 3 g/L NaCl solution. The recommended maximum voltage per cell pair is 3.0 V for safety operation. For Neosepta membranes with a flow velocity of 3 cm/s, the LCD was not observed, so it is greater than 205 A/m^2. When increasing the flow velocity to 6 cm/s, the LCD is greater than 270 A/m^2. For PES membranes with a flow velocity of 3 cm/s, the LCD exceeds 245 A/m^2. When increasing the flow velocity to 6 cm/s, the LCD is greater than 290 A/m^2. For sPES membranes with a flow velocity of 3 cm/s, the LCD is greater than 300 A/m^2. When increasing the flow velocity to 6 cm/s, the LCD is greater than 370 A/m^2. For all six tests shown in Figure 3.1, LCD was not observed, which means all experiments were performed under a safe stack voltage condition.

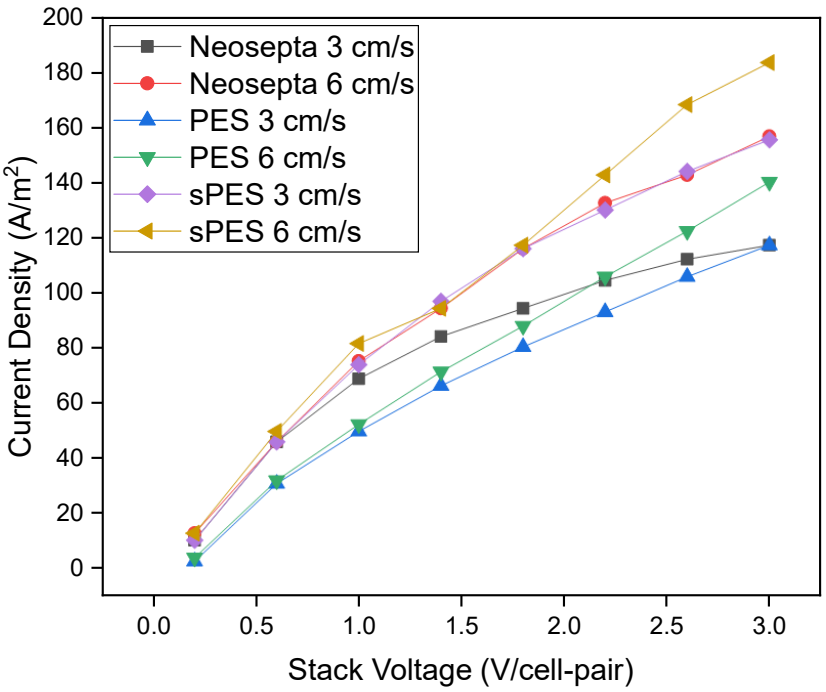

Figure 3.2: Current density of Neosepta, PES, and sPES membranes treating 3 g/L NaCl with different stack voltages per cell pair and flow velocities.

3.3.2 Electrodialysis Performance Results:

Electrodialysis performance of PES and sPES membranes was evaluated, and Neosepta commercial membranes were used as a comparison. As shown in Figure 3.3 (a), the current density of sPES is generally higher than Neosepta membranes, while the current density of PES is lower than Neosepta membranes. Thus, sPES membranes have the highest current density, which means sPES membranes have the lowest membrane resistance. Specifically, for test conditions of 3 cm/s and 0.8 V/cell-pair, the current density of PES, sPES, and Neosepta membranes was approximately 98 A/m^2, 130 A/m^2, and 100 A/m^2, respectively.

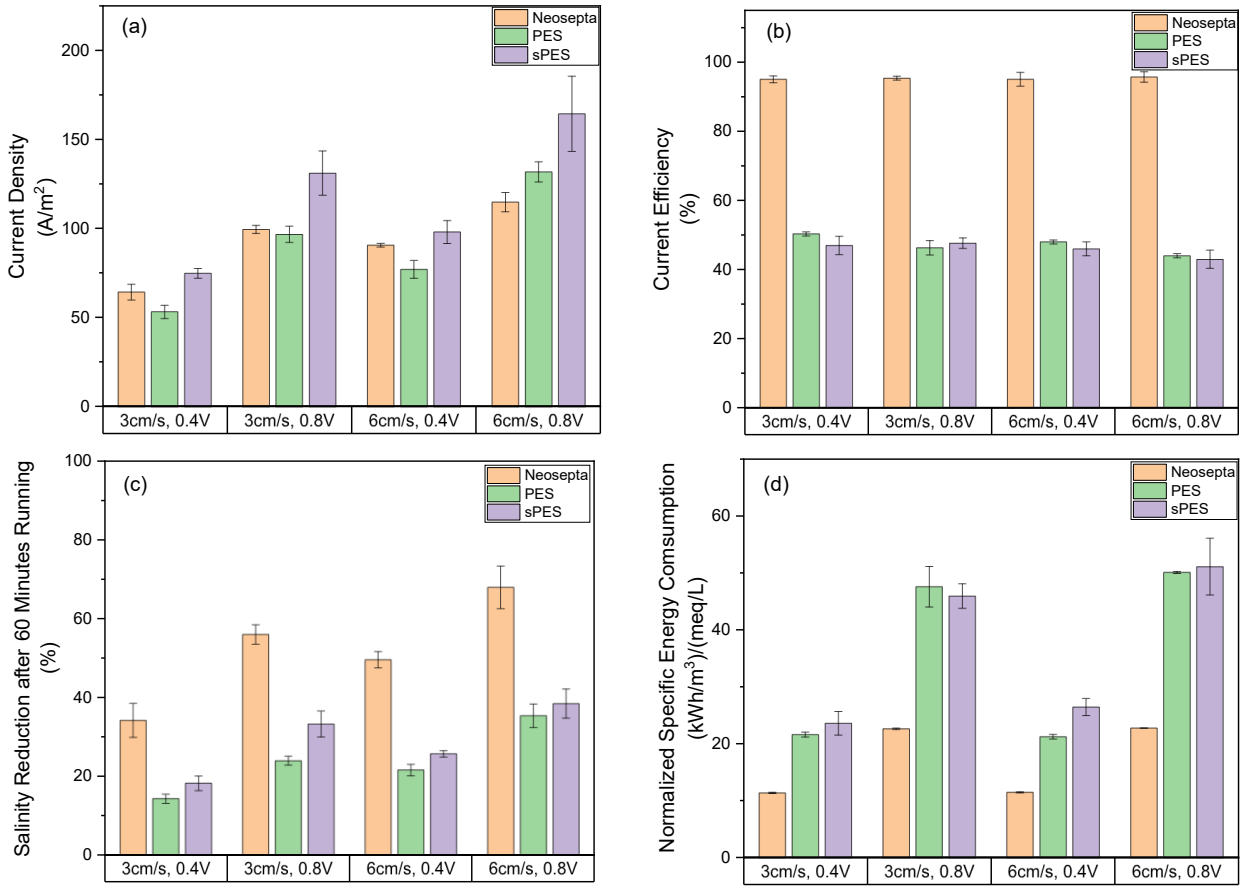

Figure 3.3: ED performances of PES and sPES membranes in different flow velocities and stack voltages per cell pair compared to Neosepta commercial membranes treating 3 g/L NaCl: (a) current density, (b) current efficiency, (c) salinity reduction after 60 minutes running, and (d) normalized specific energy consumption (nSEC).

As shown in Figure 3.3 (b), generally, the current efficiency of PES and sPES membranes is about 50% of Neosepta membranes. Specifically, for an optimized running condition of 3 cm/s and 0.8 V/cell-pair, the current efficiency of sPES membrane and PES membrane is approximately 49%, and the current efficiency of Neosepta membranes is 95%. Moreover, different applied voltages and flow velocities show little effect on current efficiency. The current efficiency of PES and sPES membranes may be because of the co-ion transport, which decreases the current efficiency greatly.

As shown in Figure 3.3 (c), generally, the salinity reduction of PES and sPES membranes

is 40% and 60% of Neosepta membranes, respectively. Specifically, for test conditions of 3 cm/s and 0.8 V/cell-pair, the salinity reduction of PES membrane is 24%, the salinity reduction of sPES membrane is 33%, and the salinity reduction of Neosepta membrane is 56%. As expected, the higher applied voltage led to a higher salinity reduction, and an increase in flow velocity resulted in a higher salinity reduction.

As shown in Figure 3.3 (d), generally, the nSEC of PES and sPES membranes is about two times that of Neosepta commercial membranes. Specifically, for test conditions of 3 cm/s and 0.8 V/cell-pair, the nSEC of PES, sPES, and Neosepta membranes was 48 (kWh/m^3)/(meq/L), 45 (kWh/m^3)/(meq/L), and 22 (kWh/m^3)/(meq/L), respectively. As expected, the higher applied voltage caused higher normalized specific energy consumption. The increase in flow velocity showed little effect on normalized specific energy consumption.

Based on further analysis, generally, it can be concluded that the salinity reduction performance of PES is 40% of Neosepta commercial membranes, while the salinity reduction performance of sPES is 60% of Neosepta commercial membranes.

3.3.3 Basic Materials Cost Estimation:

As shown in Figure 3.4, the basic materials cost of PES membranes includes the PES pellets cost and NMP cost, making the final membrane unit materials cost \$0.72/m^2.

Figure 3.4: PES membrane fabrication materials cost estimation.

As shown in Figure 3.5, the basic materials cost of sPES membranes includes the PES pellets cost, DCM cost, CSA cost, methanol cost, NMP cost, making the final sPES membrane unit materials cost \$6.21/m^2.

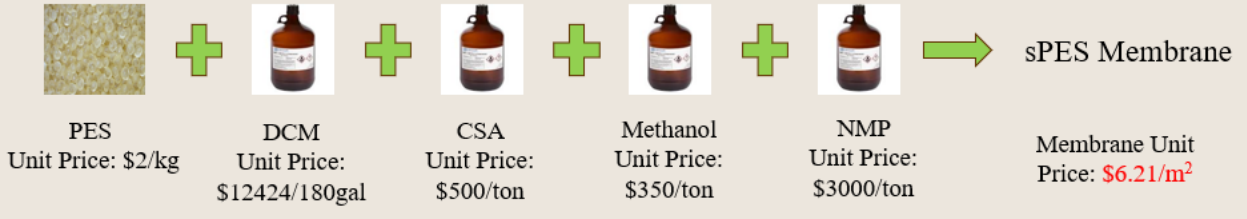

Figure 3.5: sPES membrane fabrication materials cost estimation.

3.4 CONCLUSION

In the further test results compared to Neosepta commercial membranes, the current density of PES is lower than Neosepta membranes, the current efficiency is about half of Neosepta membranes, the salinity reduction after 60 minutes running is 40% of Neosepta commercial membranes, and the normalized specific energy consumption of PES membranes is about twice of Neosepta membranes. Generally, the performance of PES membranes is 40% of Neosepta membranes. The current density of sPES is higher than Neosepta membranes, the current efficiency is about half of Neosepta membranes, the salinity reduction after 60 minutes running generally is 60% of Neosepta commercial membranes, and the normalized specific energy consumption of sPES membranes is about twice of Neosepta membranes.

Generally, the increased applied voltage increased current density, salinity reduction rate, and nSEC, as expected, but hardly affected current efficiency. The increase in flow velocity increased current density and salinity reduction rate but hardly affected current efficiency and nSEC.

The fabrication materials unit cost of PES membranes was estimated at \$0.72/m². The fabrication materials unit cost of sPES membranes was estimated at \$6.21/m². The low material

cost of PES and sPES membranes makes them cost-competitive compared to commercial membranes.

Chapter 4: Selectivity Analysis of Fabricated Ion Exchange Membranes with Real Brackish Water

4.1 INTRODUCTION

Desalination is the process of removing salts from saline water. In comparison, electrodialysis is an electric-driven technology to remove salts through ion exchange membranes, including cation and anion exchange membranes. Theoretically, cation exchange membranes would selectively only allow cations to permeate, while anion exchange membranes would only allow anions to permeate. However, in a real situation, ion exchange membranes cannot reach a hundred percent reject specific ions or permeate other ions, and there would also be some differences in permeating monovalent ions and multivalent ions. All these real-world differences make the research about selectivity meaningful.

Jiang et al. (2021) wrote a comprehensive review on the synthesis and application of ion exchange membranes. In their research, more than 30,000 papers have been published during the past twenty years (2001-2000), revealing the great interest among researchers on the topic of IEMs. Recently, there is growing interest in tailored ion-selective transport. For example, Dong et al. (2019) researched the selective removal of lead ions through ion exchange membranes. Grzegorzek et al. (2020) researched the selective removal of fluoride from multicomponent water solutions using monovalent selective IEM. Pang et al. (2020) enhanced monovalent selectivity of cation exchange membranes through adjusting the charge density on functional layers, which presented a straightforward and effective way to enhance the membrane perm-selectivity. In addition, Zhao et al. (2019) worked on synthesizing a novel anion exchange membrane with functions of enhanced monovalent anion selectivity and reduced organic fouling properties.

In this research, according to the past two chapters, sPES polymers were made by sulfonating PES polymers, and both PES and sPES membranes have some abilities to work as CEMs with the salt reduction rate of 40% and 60% of Neosepta commercial membranes approximately. This chapter focuses on evaluation of their performances with respect to ion selectivity. Neosepta commercial membranes were assessed on the same condition to be considered as a comparison. Real brackish raw water was used as the feed solution. Different flow velocities and applied voltages were considered essential parameters for their influence on the membrane selectivity performance.

4.2 MATERIAL AND METHODS

4.2.1 Materials

4.2.1.1 Brackish Water

Approximately 60 liters of brackish groundwater were collected at the Kay Bailey Hutchison (KBH) desalination plant in El Paso, Texas, on April 9, 2023. The sample had an electrical conductivity of 2.75 mS/cm a total dissolved solids (TDS) concentration of 1460 mg/L. The brackish water was analyzed by ion chromatography (IC, method detailed below) and alkalinity titration, and the composition of the raw water is listed in Table 4.1. The average sum of cations was about 26.7 meq/L, and the sum of anions was 23.4 meq/L (not including alkalinity).

Table 4.1: Compositions and ion concentrations of KBH raw water.

Parameters	Concentration (mg/L)	Concentration (meq/L)
Na^+	465	20.2
Ca^{2+}	81	4.1
Mg^{2+}	25	2.1
K^+	12	0.3
Li^+	-	-
Cl^-	710	20.0
SO_4^{2-}	163	3.4
F	-	-

4.2.1.2 Ion exchange membranes

As detailed in section 2.2.2.1, a PES dope solution was prepared by dissolving PES pellets into NMP solvent, and PES membranes were fabricated in Petri dishes by phase inversion in DI water.

According to section 2.2.2.2, the fabrication process of sPES involved two main steps. Initially, blank PES was sulfonated using CSA to increase the sulfonic acid group. This process started by dissolving blank pES in DCM, followed by the sulfonation of CSA. After quenching with methanol, the mixture underwent phase inversion by adding NMP to the sulfonated PES to form a solution, which was then poured into DI water to neutralize the pH. After drying under a fume hood, the solid sPES was ready for membrane fabrication. In the second step, a 15% sPES dope solution was prepared by dissolving dry sPES in NMP. The solution was then cast in petri dishes and allowed to evaporate for varying durations before being submerged in DI water to form the sPES membranes.

4.2.1.3 Electrodialysis (ED) desalination apparatus

A batch-cycle ED system was assembled with a pump (Cole-Parmer. Vernon Hills, IL, USA, Model:7519-00), one-liter stream reservoirs stirred by non-heating magnetic stirrers (Fisher Scientific, Waltham, MA, USA, model: Fisher 14-955-150), two pH/conductivity meters (Thermo Scientific, Bartleville, OK, USA, model: Orion Star A325), a digital scale (Meller Toledo, Columbus, OH, USA, model: XS2002S), a programmable DC power supply (B&K Precision, Yorba Linda, CA, USA, Model: 9123A), and a MicroED stack (PCCell/PCA, GmbH, Heusweiler, Germany, model: 08002-001). The active cross-sectional area of membranes assembled in the micro-ED was 7.48 cm^2 (2.8 cm*2.8 cm). The thickness of the polyester spacer was 0.45 mm used to separate the AEMs and CEMs (Hyder et al., 2021).

4.2.2 Experimental variables and value range

Experimental variables are listed in Table 4.2. The feed water for all experiments was KBH raw brackish water. The diluate stream flow velocity was controlled to either 3 cm/s or 6 cm/s. The stack voltage was set to 0.4 V/cell-pair or 0.8 V/cell-pair. There are three membrane combinations for comparison: PES and Neosepta AMX76, sPES and Neosepta AMX76, and Neosepta CMX76 and AMX76.

Table 4.2: Experimental variables and value ranges.

Variables	Values
Feed water	KBH raw brackish water
Flow velocity of diluate stream	3, 6 cm/s
Stack voltage	0.4, 0.8 V/cell-pair
Combination of membranes	i) PES & Neosepta AMX76 ii) sPES & Neosepta AMX76 iii) Neosepta CMX76 & AMX76

4.2.3 Ion chromatography (IC) analysis

IC analysis was performed with simultaneous IC instruments and corresponding software. The cation analysis was conducted with a Dionex Aquion (S/N: 180946142) instrument with a column model of Dionex IonPacTM CS16 RFICTM and a 5 mm × 250 mm analytical column (Thermo Scientific). The anion analysis was conducted with a Dionex Integrion (HPIC) instrument with a column model of Dionex IonPacTM AS18 RFICTM and a 4 mm × 250 mm analytical column (Thermo Scientific). The eluents for the IC analysis were 47 mM methanesulfonic acid (MSA) solution and 0.3 M KOH, respectively.

4.2.4 Ion selectivity testing procedure

Feed water preparation. Collect natural brackish water from KBH. Assemble the membrane stack, set voltage, set flow velocity, and set load KBH water. Equal volumes of diluate and concentrate represented a nominal recovery of 50%.

Collect samples. Draw 1 mL of feed water before engaging the power supply to the ED stack. Engage the power supply and run the ED for 1 to 2 hours. During operation, collect water samples when there is 10%, 20%, 30%, 40%, 50%, 60%, and 70% conductivity reduction in diluate. Each running condition was repeated in triplicate.

IC test of samples. Dilute the collected water samples so that the conductivity falls into the 400-1000 μs/cm range. Perform IC analyses to determine the concentration of each ion.

Selectivity analysis. Calculate the relative transport number (RTN) to evaluate the selectivity performance. The selectivity performance was focused on major ions, especially Na^+, Ca^{2+}, Cl^-, SO_4^{2-}.

4.2.5 Calculation Methods

4.2.5.1 Limiting Current Density (LCD)

Refer to Section 3.2.2.2 Limiting Current Density (LCD).

4.2.5.2 Relative transport number (RTN)

The relative transport number for an ion (X) relative to another ion (Y) can be calculated from the following equation [17]:

$$RTN_Y^X = \frac{R_X}{R_Y} \tag{4.1}$$

Where, R_X and R_Y indicate the concentration reduction of X and Y ion, respectively in the diluate stream.

4.3 RESULT AND DISCUSSION

4.3.1 Limiting Current Density (LCD)

As shown in Figure 4.1, the current density of Neosepta, PES, and sPES membranes

increased with the increase of stack voltage applied to each cell pair. Considering the safety issue, the largest voltage to be applied of the stack voltage per cell pair is 3.0 V. From Figure 4.1, Neosepta membranes, for KBH raw water feed solution with a flow velocity of 3 cm/s, the LCD was about 120 A/m^2 since the current density almost reached an equilibrium. When increasing the flow velocity to 6 cm/s, the LCD was larger than 160 A/m^2. From Figure 4.1 PES membranes, for KBH raw water feed solution with a flow velocity of 3 cm/s, the LCD was more than 120 A/m^2. When increasing the flow velocity to 6 cm/s, the LCD was more than 140 A/m^2. From Figure 4.1 sPES membranes, for KBH raw water feed solution with a flow velocity of 3 cm/s, the LCD was more than 155 A/m^2. When increasing the flow velocity to 6 cm/s, the LCD was more than 185 A/m^2.

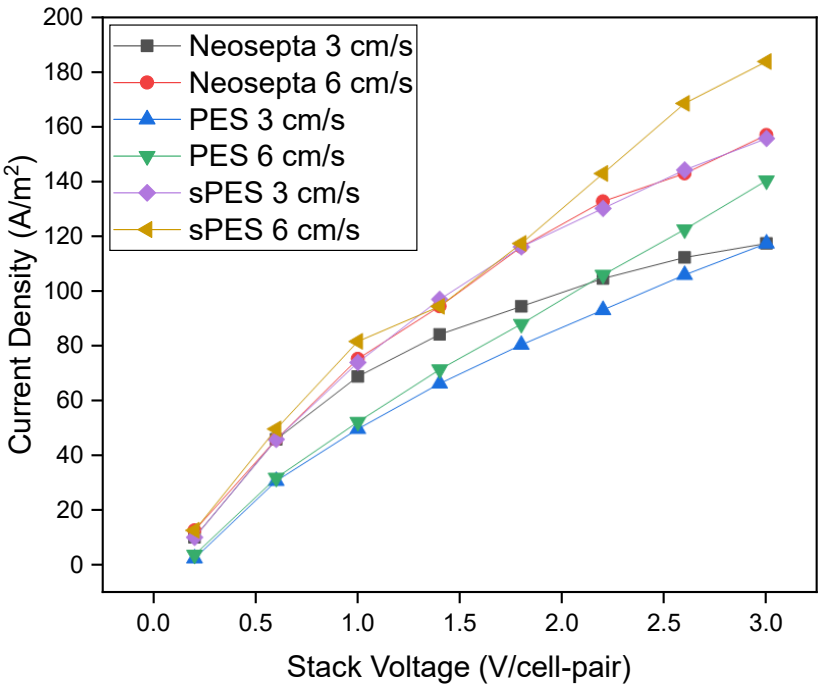

Figure 4.1: Current density of Neosepta, PES, and sPES membranes in KBH raw water with the increase of stack voltages per cell pair and with different flow velocities.

4.3.2 Evaluation of removal ratio of dominant monovalent and divalent ions

As shown in Table 4.1, the predominant monovalent ions are sodium (Na^+) and chloride (Cl^-), while the predominant divalent ions are calcium (Ca^{2+}) and sulfate (SO_4^{2-}). If a membrane demonstrated no selectivity, then the concentration of the ions would be reduced at the same rate as the bulk conductivity reduction ratio.

From Figure 4.2, generally, the removal ratio of each ion increases with the increase of bulk conductivity reduction. As shown in Figure 4.2, based on the same flow velocity of 3 cm/s, the different applied stack voltages and membrane combinations affect the ion reduction. As shown in Figure 4.2 (a), the calcium removal ratio increases with increased bulk conductivity reduction in diluate. For all the three membrane combinations, the removal ratio of a lower applied stack voltage has a higher removal ratio than the one of a higher applied stack voltage. As shown in Figure 4.2 (b), the removal ratio of sodium shows less sensitivity to stack voltage than calcium, chloride, and sulfate. As shown in Figure 4.2 (c), for the Neosepta membranes, the higher stack voltage brings higher sulfate removal ratio than a lower stack voltage. While for the fabricated PES and sPES membrane combinations, there is no removal ratio of sulfate. The reason of no sulfate removal is probably because of the co-ion transport happened in the PES and sPES membranes, the fabricated PES and sPES membranes cannot reject divalent sulfate ions. As shown in Figure 4.2 (d), for Neosepta membranes, the removal ratio of sodium shows less sensitivity to stack voltage. However, for the fabricated PES and sPES membranes, the chloride removal ratio of a lower stack voltage is higher than the one of a higher stack voltage. And sPES membrane combination has a better chloride removal performance than PES membrane combination.

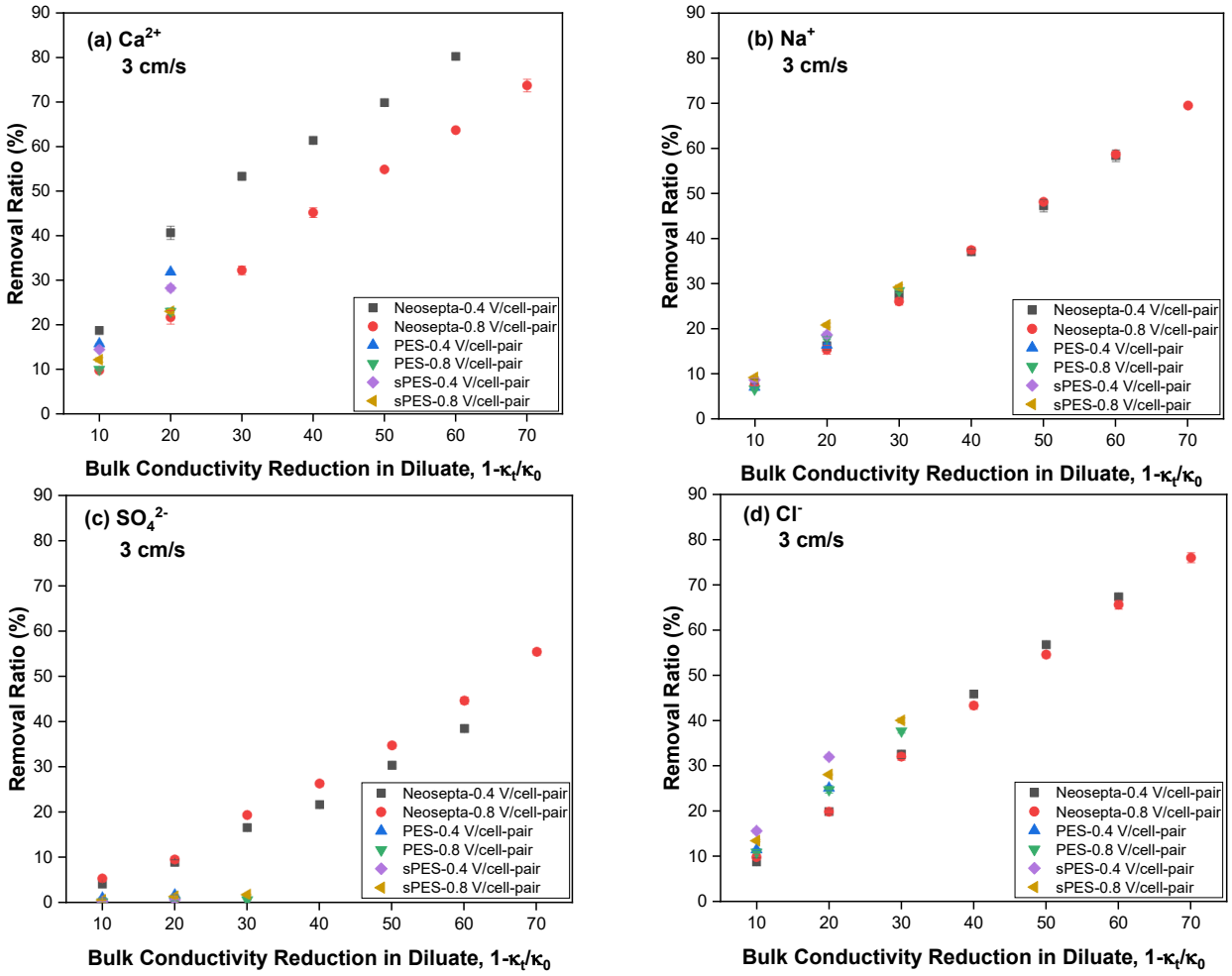

Figure 4.2: Effect of stack voltage on removal ratio of Ca^{2+}, Na^{+}, SO_4^{2-}, and Cl^{-} ions (parts a through d, respectively) from KBH raw brackish feed water with the increase of bulk conductivity reduction in diluate when the flow velocity was 3 cm/s.

Thus, the different applied stack voltage would affect the permeability of calcium, sulfate and chloride, but it would not affect sodium that much. Calcium and chloride would be removed better in a lower stack voltage, while sulfate would be removed better in a higher stack voltage. Moreover, because of the co-ion transport, there is no sulfate removal for PES and sPES membrane combinations.

As shown in Figure 4.3, the effect of different flow velocities on the removal performance of predominant monovalent and divalent ions from KBH raw brackish water is based

on the same applied stack voltage of 0.8 V/cell-pair. As shown in Figure 4.3 (a), the calcium increases with the increase of the bulk conductivity reduction in diluate. And the removal ratio of a higher flow velocity is higher than the one of a lower flow velocity for calcium removal. As shown in Figure 4.3 (b), based on the same applied stack voltage, the sodium removal is relatively insensitive to different flow velocities and membrane combinations. As shown in Figure 4.3 (c), the sulfate removal of a lower flow velocity is better than of a higher flow velocity for Neosepta membrane combination. While for the fabricated PES and sPES membrane combiantions, there is almost no sulfate removal. This may be because of the co-ion transport that happened in the fabricated membranes. As shown in Figure 4.3 (d), generally, based on the same applied stack voltage, the chloride removal is relatively insensitive to different flow velocities and membrane combination. For Neosepta membrane combination, there is only a slight difference that the removal ratio of a higher flow velocity is slightly higher than the one of a lower flow velocity.

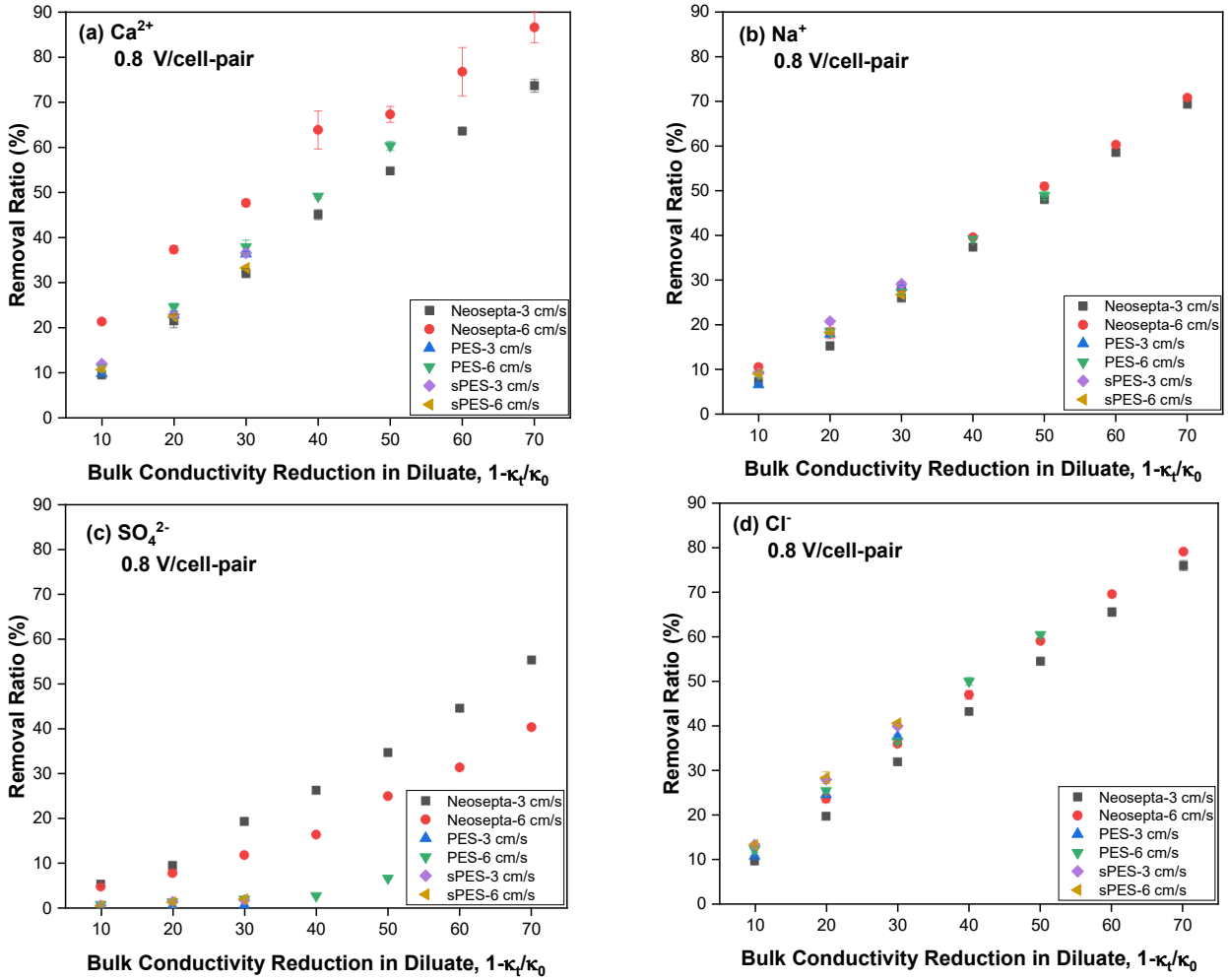

Figure 4.3: Effect of flow velocity on removal ratio of Ca^{2+}, Na^{+}, SO_4^{2-}, and Cl^{-} ions (parts a through d, respectively) from KBH raw brackish feed water with the increase of bulk conductivity reduction in diluate when the applied stack voltage was 0.8 V/cell-pair.

Thus, based on the same applied stack voltage, the different flow velocities would affect the permeability of calcium, sulfate, and chloride, but it would not affect sodium that much. A high flow velocity benefits the removal of calcium and chloride, and a lower flow velocity benefits the removal of sulfate. Moreover, because of the co-ion transport, there is no sulfate removal for PES and sPES membrane combinations.

4.3.3 Evaluation of relative transport number between divalent and monovalent ions

As shown in Figure 4.4 (a) and (b), the relative transport number (RTN) of calcium to sodium decreases toward 1.0 with the increase of bulk conductivity reduction in diluate. As shown in Figure 4.4 (a), when the flow velocity is 3 cm/s, the RTN of the lower stack voltage is higher than the RTN of higher stack voltage, which means that in lower stack voltage running conditions, all three membrane combinations show higher membrane selectivity feature, which is between 1.2 to 2.5. As shown in Figure 4.4 (b), when the stack voltage is 0.8 V/cell-pair, the RTN of the higher flow velocity is more elevated than the RTN of low flow velocity, meaning membrane combinations show a better selectivity feature in a higher flow velocity. Generally, the selectivity of these three membrane combinations between calcium and sodium is not apparent. As shown in Figure 4.4 (c) and (d), the relative transport number (RTN) of sulfate to chloride increases toward 1.0 with the increase of bulk conductivity reduction in diluate. As shown in Figure 4.4 (c), when the flow velocity is 3 cm/s, the RTN of Neosepta is about 0.5 to 0.7, and a higher stack voltage brings a slightly higher RTN than a lower stack voltage. While the RTN of PES membrane combination and sPES membrane combination is less than 0.1, which means that PES and sPES membrane combinations remove chloride efficiently while not removing sulfate. As shown in Figure 4.4 (d), when the stack voltage is 0.8 V/cell-pair, the RTN of Neosepta membrane combination is about 0.3 to 0.7, and a lower flow velocity brings higher RTN than higher flow velocity, which means a higher flow velocity results in a greater membrane selectivity between sulfate and chloride. While the RTN of PES and sPES membrane combinations are less than 0.1, which means that PES and sPES membrane combinations remove chloride efficiently while not removing sulfate.

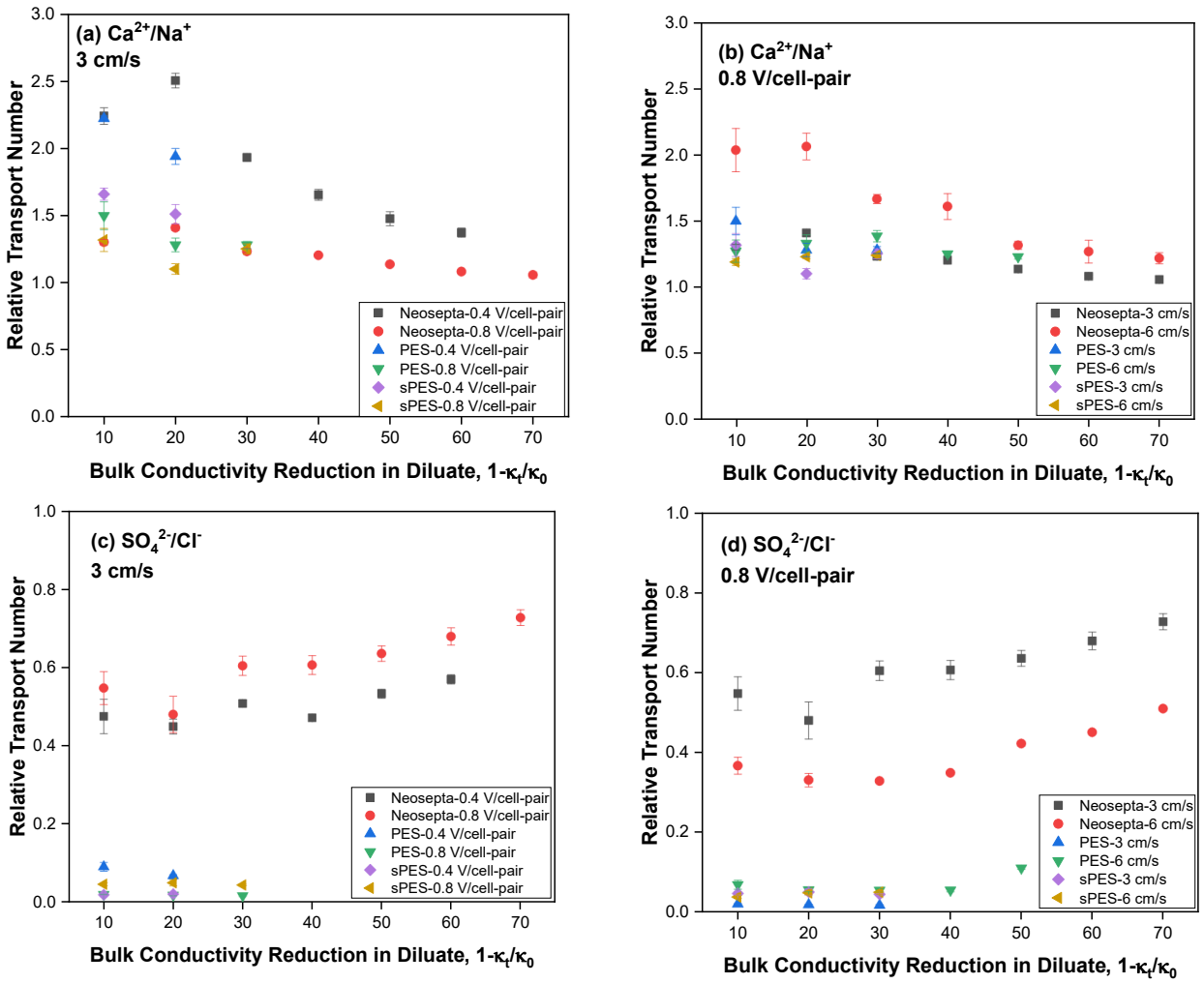

Figure 4.4: Effect of stack voltage and flow velocity on relative transport number of divalent ions against monovalent ions: Ca^{2+} vs Na^{+} (a, b) and SO_4^{2-} vs Cl^{-} (c, d) from KBH raw brackish feed water.

Thus, PES and sPES membrane combinations generally have significant selectivity function between sulfate and chloride ions but almost no selectivity between calcium and sodium ions. It is probably because of the co-ion transport that happened in the fabricated PES and sPES membranes. The fabricated membranes can reject monovalent ions like chloride, while not able to reject divalent ions like sulfate. This co-ion transport can also be proved by the low current efficiency of the fabricated membranes. These Neosepta membranes do not show any apparent selectivity in either situation.

4.4 CONCLUSION

From all the results and analysis shown above, about the evaluation of membrane selectivity performances of three ion exchange membrane combinations in real brackish water, we can draw some conclusions shown below:

Firstly, when the diluate bulk conductivity decreases, the concentration of those predominant ions is reduced at approximately the same rate as the bulk conductivity reduction ratio. Neosepta membranes show a better ion reduction rate with an increased bulk conductivity reduction rate.

Secondly, running conditions like stack voltages and flow velocities have a noticeable effect on the removal rate of divalent ions (calcium and sulfate). Still, they show limited impact on removing monovalent ions (sodium and chloride).

Thirdly, PES and sPES membrane combinations show a prominent selectivity feature of sulfate to chloride: they have an RTN of approximately 0.1. Different running conditions, like flow velocities and stack voltages, show little effect on their selectivity function.

Lastly, the RTN of calcium to sodium decreases with increased bulk conductivity reduction rate in diluate. However, the RTN of sulfate to chloride increases with the increase of bulk conductivity reduction rate in diluate.

Chapter 5: General Conclusions and Recommendations

5.1 General Conclusions

After reviewing relevant current literature, there have been long histories of the research of ED, over a similar timeframe as RO. However, the public application of ED is much less than RO. One significant challenge limiting the broad application of ED is the cost of IEMs compared with RO membranes. Although many research papers have been published, the industrial development of IEMs for ED desalination is very limited. In addition, the selectivity research of IEMs is also significant. Thus, to bring human society great benefits to access potable water with ED desalination application, the fabrication of inexpensive and high perm-selective IEMs would be very valuable. In this research, there are three major projects to reach the goal.

The first project (Ch. 2) aimed to fabricate inexpensive IEMs, including PES and sPES cation exchange membranes. Since PES polymer is a very inexpensive material, it could decrease the material costs of membrane fabrication. With different solvent evaporation times, the fabricated membranes showed different electrodialysis performance. Membranes with the best performance were selected for subsequent ED tests, and Neosepta commercial membranes were used as comparisons. The fabricated IEMs were characterized with FTIR, AFM, and XPS. Sulfonation degree (SD) and ion exchange capacity (IEC) were analyzed, as well. It can be concluded that the PES membranes and sPES membranes with the best performance were achieved with evaporation times of 3 hr and 1 hr, respectively. The salinity reduction after 60 minutes running for PES and sPES membranes were 24% and 33%, respectively. And from the characteristics of AFM, FTIR-ATR, and XPS analysis, the effect of sulfonation process did increase the degree of sulfonation. This research contributed to the possibility of using PES polymers for the IEMs fabrication for ED application. And the increased performance of sPES

membranes compared with PES membranes brought inspirations that the IEMs made with PES polymers can be enhanced with certain treatment, which provided references for the development of IEMs for ED.

The second project (Ch. 3) aimed to evaluate the fabricated IEMs ED performance compared with Neosepta membranes. Different running parameters were considered and used to see the influence on the ED membranes' performance, including the feed water quality (3 g/L NaCl solution), applied stack voltage per cell-pair (0.4 V and 0.8 V), flow velocity (3 cm/s and 6 cm/s), and different membranes combinations. All experiments were conducted in triplicate except LCD results. The ED performances of IEMs were evaluated by determining the following metrics: limiting current density (LCD), current density (CD), current efficiency (CE), salinity reduction (SR), normalized specific energy consumption (nSEC). It can be concluded that the salinity reduction after 60 minutes of running of PES and sPES membranes is approximately 40% and 60%, respectively, of Neosepta membranes. Moreover, the increased applied voltage increased current density, salinity reduction rate, and nSEC, as expected, but hardly affected current efficiency. The increase in flow velocity increased current density and salinity reduction rate but hardly affected current efficiency and nSEC. This research contributed to the findings of how ED running conditions including flow velocities and applied stack voltages affected the ED performance. In addition, the evaluation of fabricated PES and sPES ED performances also contributed to the field of IEMs for ED application with more references.

The third project (Ch. 4) aimed to evaluate the fabricated IEMs selectivity performance toward major ions in real brackish water. KBH raw water was collected and used for this part of the research, the raw water had an electrical conductivity of 2.75 mS/cm, corresponding TDS of about 1500 mg/L. The selectivity was evaluated by adjusting the feed water (KBH raw water),

flow velocity (3 cm/s and 6 cm/s), applied stack voltage per cell-pair (0.4 V and 0.8 V), and the membrane combinations. The concentration reduction of major ions and relative transport number (RTN) was measured as the evaluation metric. Ion chromatography (IC) equipment was used to measure the concentration of ions in water samples. All the experiments were performed in triplicate (except LCD results), and commercial Neosepta membranes were used as a comparison in the selectivity evaluation. It can be concluded that running conditions like stack voltages and flow velocities had a noticeable effect on the removal of divalent ions (calcium and sulfate) while they showed limited impact on removing monovalent ions (sodium and chloride). In addition, the PES and sPES membrane combinations showed a prominent selectivity feature of sulfate to chloride: they had an RTN of approximately 0.1, which may result from the co-ion transport of sulfate. This research contributed to the analysis of the effect of running conditions including flow velocities and applied stack voltages on the membrane selectivity feature of IEMs. Moreover, the low RTN number of 0.1 of sulfate to chloride and the real brackish water as feed solution may bring more valuable reference for the ED practical application.

This research contributed to the field of ED by the fabrication and characterization on the research of inexpensive IEMs. PES polymer was used as the main material for PES and sPES cation exchange membranes fabrication. For the characterization of the fabricated membranes, FTIR-ATR, AFM, XPS methods were applied, which indicated the difference of sulfonation made on the fabricated sPES membranes. In addition, IEC and DS were also calculated to show the increase of sulfonic acid group content in sPES membranes compared to PES membranes. All these provided a bright future of IEMs fabrication for ED desalination application. This research also contributed to the field of ED by the systematic ED evaluation methodology. By considering the different running conditions, including feed water solutions, flow velocity, applied stack

voltage, etc., the ED experiments were operated. Moreover, performance evaluation metrics were used for the ED evaluation, which included current density, current efficiency, salinity reduction, specific energy consumption, limiting current density, etc. Finally, this research contributed to the ED area by illustrating the importance of evaluation with real brackish feed water. The data and analysis results from real brackish feed water brought strong references for the practical application of ED desalination, making a connection between laboratory research and real work applications.

5.2 RECOMMENDATIONS FOR FUTURE WORK

Based on this dissertation research, there are several places that can be improved for future research. Firstly, the improvement of IEMs' current efficiency. The IEMs fabricated in this research showed a current efficiency around 50%, which was not good enough compared to most commercial IEMs. It is probably because the sulfonation time was only 1 hr. For future research, it is recommended that the sulfonation time be extended to 24 hr or longer so that the current efficiency may be increased. Secondly, the selectivity analysis can be performed with more sources of real brackish water rather than one source. This may enhance the persuasiveness and comparativeness of results. Thirdly, a comprehensive cost analysis is encouraged to be performed to make great reference for the practical application of ED technology.

Reference

Abdu, S., Martí-Calatayud, M. C., Wong, J. E., García-Gabaldón, M., & Wessling, M. (2014). Layer-by-layer modification of cation exchange membranes controls ion selectivity and water splitting. *ACS Applied Materials and Interfaces*, *6*(3), 1843–1854. https://doi.org/10.1021/am4048317

Afsar, N. U., Shehzad, M. A., Irfan, M., Emmanuel, K., Sheng, F., Xu, T., Ren, X., Ge, L., & Xu, T. (2019). Cation exchange membrane integrated with cationic and anionic layers for selective ion separation via electrodialysis. *Desalination*, *458*(February), 25–33. https://doi.org/10.1016/j.desal.2019.02.004

Ahdab, Y. D., Schücking, G., Rehman, D., & Lienhard, J. H. (2021). Treatment of greenhouse wastewater for reuse or disposal using monovalent selective electrodialysis. *Desalination*, *507*(December 2020), 115037. https://doi.org/10.1016/j.desal.2021.115037

Ahmad, M., Tang, C., Yang, L., Yaroshchuk, A., & Bruening, M. L. (2019). Layer-by-layer modification of aliphatic polyamide anion-exchange membranes to increase Cl−/SO42− selectivity. *Journal of Membrane Science*, *578*(February), 209–219. https://doi.org/10.1016/j.memsci.2019.02.018

Akther, N., Sodiq, A., Giwa, A., Daer, S., Arafat, H. A., & Hasan, S. W. (2015). Recent advancements in forward osmosis desalination: A review. *Chemical Engineering Journal*, *281*, 502–522. https://doi.org/10.1016/j.cej.2015.05.080

Al-Amshawee, S., Yunus, M. Y. B. M., Azoddein, A. A. M., Hassell, D. G., Dakhil, I. H., & Hasan, H. A. (2020). Electrodialysis desalination for water and wastewater: A review. *Chemical Engineering Journal*, *380*(July 2019). https://doi.org/10.1016/j.cej.2019.122231

Alklaibi, A. M., & Lior, N. (2005). Membrane-distillation desalination: Status and potential.

Desalination, *171*(2), 111–131. https://doi.org/10.1016/j.desal.2004.03.024

Avci, A. H., Messana, D. A., Santoro, S., Tufa, R. A., Curcio, E., Di Profio, G., & Fontananova, E. (2020). Energy harvesting from brines by reverse electrodialysis using nafion membranes. *Membranes*, *10*(8), 1–16. https://doi.org/10.3390/membranes10080168

Biesheuvel, P. M., Porada, S., Elimelech, M., & Dykstra, J. E. (2021). *Tutorial review of Reverse Osmosis and Electrodialysis*. *647*(January). https://doi.org/10.1016/j.memsci.2021.120221

Campione, A., Gurreri, L., Ciofalo, M., Micale, G., Tamburini, A., & Cipollina, A. (2018). Electrodialysis for water desalination: A critical assessment of recent developments on process fundamentals, models and applications. *Desalination*, *434*(October 2017), 121–160. https://doi.org/10.1016/j.desal.2017.12.044

Cao, X., Tang, M., Liu, F., Nie, Y., & Zhao, C. (2010). Immobilization of silver nanoparticles onto sulfonated polyethersulfone membranes as antibacterial materials. *Colloids and Surfaces B: Biointerfaces*, *81*(2), 555–562. https://doi.org/10.1016/j.colsurfb.2010.07.057

Chakraborty, I., Das, S., Dubey, B. K., & Ghangrekar, M. M. (2020). Novel low cost proton exchange membrane made from sulphonated biochar for application in microbial fuel cells. *Materials Chemistry and Physics*, *239*(August 2019), 122025. https://doi.org/10.1016/j.matchemphys.2019.122025

Chen, S., Wang, H., Zhang, J., Lu, S., & Xiang, Y. (2020). Effect of side chain on the electrochemical performance of poly (ether ether ketone) based anion-exchange membrane: A molecular dynamics study. *Journal of Membrane Science*, *605*(April), 118105. https://doi.org/10.1016/j.memsci.2020.118105

Cheng, C., White, N., Shi, H., Robson, M., & Bruening, M. L. (2014). Cation separations in electrodialysis through membranes coated with polyelectrolyte multilayers. *Polymer*, *55*(6),

1397–1403. https://doi.org/10.1016/j.polymer.2013.12.002

Cohen, B., Lazarovitch, N., & Gilron, J. (2018). Upgrading groundwater for irrigation using monovalent selective electrodialysis. *Desalination*, *431*(June 2017), 126–139. https://doi.org/10.1016/j.desal.2017.10.030

Di Virgilio, M., Basso Peressut, A., Arosio, V., Arrigoni, A., Latorrata, S., & Dotelli, G. (2023). Functional and Environmental Performances of Novel Electrolytic Membranes for PEM Fuel Cells: A Lab-Scale Case Study. *Clean Technologies*, *5*(1), 74–93. https://doi.org/10.3390/cleantechnol5010005

Dong, Q., Guo, X., Huang, X., Liu, L., Tallon, R., Taylor, B., & Chen, J. (2019). Selective removal of lead ions through capacitive deionization: Role of ion-exchange membrane. *Chemical Engineering Journal*, *361*(October 2018), 1535–1542. https://doi.org/10.1016/j.cej.2018.10.208

Eke, J., Yusuf, A., Giwa, A., & Sodiq, A. (2020). The global status of desalination: An assessment of current desalination technologies, plants and capacity. *Desalination*, *495*(August), 114633. https://doi.org/10.1016/j.desal.2020.114633

Elsaid, K., Sayed, E. T., Abdelkareem, M. A., Mahmoud, M. S., Ramadan, M., & Olabi, A. G. (2020). Environmental impact of emerging desalination technologies: A preliminary evaluation. *Journal of Environmental Chemical Engineering*, *8*(5), 104099. https://doi.org/10.1016/j.jece.2020.104099

Fan, H., Xu, Y., Zhao, F., Chen, Q. B., Wang, D., & Wang, J. (2023). A novel porous asymmetric cation exchange membrane with thin selective layer for efficient electrodialysis desalination. *Chemical Engineering Journal*, *472*(May), 144856. https://doi.org/10.1016/j.cej.2023.144856

Fritzmann, C., Löwenberg, J., Wintgens, T., & Melin, T. (2007). State-of-the-art of reverse osmosis desalination. *Desalination*, *216*(1–3), 1–76. https://doi.org/10.1016/j.desal.2006.12.009

Gahlot, S., Sharma, P. P., Gupta, H., Kulshrestha, V., & Jha, P. K. (2014). Preparation of graphene oxide nano-composite ion-exchange membranes for desalination application. *RSC Advances*, *4*(47), 24662–24670. https://doi.org/10.1039/c4ra02216e

Gahlot, S., Yadav, V., Sharma, P. P., & Kulshrestha, V. (2019). Zn-MOF@SPES composite membranes: synthesis, characterization and its electrochemical performance. *Separation Science and Technology (Philadelphia)*, *54*(3), 377–385. https://doi.org/10.1080/01496395.2018.1505916

Generous, M. M., Qasem, N. A. A., Akbar, U. A., & Zubair, S. M. (2021). Techno-economic assessment of electrodialysis and reverse osmosis desalination plants. *Separation and Purification Technology*, *272*(May), 118875. https://doi.org/10.1016/j.seppur.2021.118875

Generous, M. M., Qasem, N. A. A., & Zubair, S. M. (2020). The significance of modeling electrodialysis desalination using multi-component saline water. *Desalination*, *496*(January), 114347. https://doi.org/10.1016/j.desal.2020.114347

Grebenyuk, V. D., & Grebenyuk, O. V. (2002). *Electrodialysis : From an Idea to Realization* *. *38*(8), 806–809.

Grzegorzek, M., Majewska-Nowak, K., & Ahmed, A. E. (2020). Removal of fluoride from multicomponent water solutions with the use of monovalent selective ion-exchange membranes. *Science of the Total Environment*, *722*, 137681. https://doi.org/10.1016/j.scitotenv.2020.137681

Guan, R., Zou, H., Lu, D., Gong, C., & Liu, Y. (2005). Polyethersulfone sulfonated by

chlorosulfonic acid and its membrane characteristics. *European Polymer Journal*, *41*(7), 1554–1560. https://doi.org/10.1016/j.eurpolymj.2005.01.018

Hand, S., Guest, J. S., & Cusick, R. D. (2019). Technoeconomic Analysis of Brackish Water Capacitive Deionization: Navigating Tradeoffs between Performance, Lifetime, and Material Costs. *Environmental Science and Technology*, *53*(22), 13353–13363. https://doi.org/10.1021/acs.est.9b04347

He, S., Lin, Y., Ma, H., Jia, H., Liu, X., & Lin, J. (2016). Preparation of sulfonated poly(ether ether ketone) (SPEEK) membrane using ethanol/water mixed solvent. *Materials Letters*, *169*, 69–72. https://doi.org/10.1016/j.matlet.2016.01.099

Honarparvar, S., & Reible, D. (2020). Modeling multicomponent ion transport to investigate selective ion removal in electrodialysis. *Environmental Science and Ecotechnology*, *1*(October 2019), 100007. https://doi.org/10.1016/j.ese.2019.100007

Hyder, A. G., Morales, B. A., Cappelle, M. A., Percival, S. J., Small, L. J., Spoerke, E. D., Rempe, S. B., & Walker, W. S. (2021). Evaluation of electrodialysis desalination performance of novel bioinspired and conventional ion exchange membranes with sodium chloride feed solutions. *Membranes*, *11*(3). https://doi.org/10.3390/membranes11030217

Irfan, M., Wang, Y., & Xu, T. (2020). Novel electrodialysis membranes with hydrophobic alkyl spacers and zwitterion structure enable high monovalent/divalent cation selectivity. *Chemical Engineering Journal*, *383*(August 2019), 123171. https://doi.org/10.1016/j.cej.2019.123171

Jain, A., Weathers, C., Kim, J., Meyer, M. D., Walker, W. S., Li, Q., & Verduzco, R. (2019). Self assembled, sulfonated pentablock copolymer cation exchange coatings for membrane capacitive deionization. *Molecular Systems Design and Engineering*, *4*(2), 348–356. https://doi.org/10.1039/c8me00115d

Jiang, S., Sun, H., Wang, H., Ladewig, B. P., & Yao, Z. (2021). A comprehensive review on the synthesis and applications of ion exchange membranes. *Chemosphere*, *282*(March), 130817. https://doi.org/10.1016/j.chemosphere.2021.130817

Jones, E., Qadir, M., van Vliet, M. T. H., Smakhtin, V., & Kang, S. mu. (2019). The state of desalination and brine production: A global outlook. *Science of the Total Environment*, *657*, 1343–1356. https://doi.org/10.1016/j.scitotenv.2018.12.076

Káňavová, N., Machuča, L., & Tvrzník, D. (2014). Determination of limiting current density for different electrodialysis modules. *Chemical Papers*, *68*(3), 324–329. https://doi.org/10.2478/s11696-013-0456-z

Khan, M. I., Zheng, C., Mondal, A. N., Hossain, M. M., Wu, B., Emmanuel, K., Wu, L., & Xu, T. (2017). Preparation of anion exchange membranes from BPPO and dimethylethanolamine for electrodialysis. *Desalination*, *402*, 10–18. https://doi.org/10.1016/j.desal.2016.09.019

KIM, I. C., CHOI, J. G., & TAK, T. M. (1999). Sulfonated Polyethersulfone by Heterogeneous Method and Its Membrane Performances. *Journal of Applied Polymer Science*, *74*(8), 2046–2205.

Klaysom, C., Ladewig, B. P., Lu, G. Q. M., & Wang, L. (2011). Preparation and characterization of sulfonated polyethersulfone for cation-exchange membranes. *Journal of Membrane Science*, *368*(1–2), 48–53. https://doi.org/10.1016/j.memsci.2010.11.006

Klaysom, C., Moon, S. H., Ladewig, B. P., Lu, G. Q. M., & Wang, L. (2011). Preparation of porous ion-exchange membranes (IEMs) and their characterizations. *Journal of Membrane Science*, *371*(1–2), 37–44. https://doi.org/10.1016/j.memsci.2011.01.008

Krishna, B. A., Lindhoud, S., & de Vos, W. M. (2021). Hot-pressed polyelectrolyte complexes as novel alkaline stable monovalent-ion selective anion exchange membranes. *Journal of*

Colloid and Interface Science, *593*, 11–20. https://doi.org/10.1016/j.jcis.2021.02.077

Krol, J. J., Wessling, M., & Strathmann, H. (1999). Concentration polarization with monopolar ion exchange membranes: Current-voltage curves and water dissociation. *Journal of Membrane Science*, *162*(1–2), 145–154. https://doi.org/10.1016/S0376-7388(99)00133-7

Landolt-Börnstein: Numerical Values and Functions. 6th Edition, Volume II, Properties of Matter in their States of Aggregation. Part 7, Electrical Properties II (Electrochemical Systems). Springer Verlag, Berlin-Göttingen-Heidelberg 1960. 959 pages. Price: DM 478, -, Zeitschrift für Elektrochemie, reports of the Bunsen Society for Phys. Chemistry. 66 (1962) 74-74

Lee, H. J., Sarfert, F., Strathmann, H., & Moon, S. H. (2002). Designing of an electrodialysis desalination plant. *Desalination*, *142*(3), 267–286. https://doi.org/10.1016/S0011-9164(02)00208-4

Lee, H. J., Strathmann, H., & Moon, S. H. (2006). Determination of the limiting current density in electrodialysis desalination as an empirical function of linear velocity. *Desalination*, *190*(1–3), 43–50. https://doi.org/10.1016/j.desal.2005.08.004

Li, R., Liu, L., Zhang, Y., & Yang, F. (2016). Preparation of a nano-MnO2 surface-modified reduced graphene oxide/PVDF flat sheet membrane for adsorptive removal of aqueous Ni(II). *RSC Advances*, *6*(25), 20542–20550. https://doi.org/10.1039/c5ra20776b

Li, Z., Ma, Z., Xu, Y., Wang, X., Sun, Y., Wang, R., Wang, J., Gao, X., & Gao, J. (2018). Developing homogeneous ion exchange membranes derived from sulfonated polyethersulfone/N-phthaloyl-chitosan for improved hydrophilic and controllable porosity. *Korean Journal of Chemical Engineering*, *35*(8), 1716–1725. https://doi.org/10.1007/s11814-018-0064-2

Liao, J., Yu, X., Pan, N., Li, J., Shen, J., & Gao, C. (2019). Amphoteric ion-exchange membranes with superior mono-/bi-valent anion separation performance for electrodialysis applications. *Journal of Membrane Science*, *577*(February), 153–164. https://doi.org/10.1016/j.memsci.2019.01.052

Mabrouk, W., Lafi, R., Fauvarque, J. F., Hafiane, A., & Sollogoub, C. (2021). New ion exchange membrane derived from sulfochlorated polyether sulfone for electrodialysis desalination of brackish water. *Polymers for Advanced Technologies*, *32*(1), 304–314. https://doi.org/10.1002/pat.5086

Mayyas, A., Ruth, M., Pivovar, B., Bender, G., Wipke, K., Mayyas, A., Ruth, M., Pivovar, B., Bender, G., & Wipke, K. (2019). Manufacturing Cost Analysis for Proton Exchange Membrane Water Electrolyzers. *National Renewable Energy Laboratory*, *August*, 65. https://www.nrel.gov/docs/fy10osti/72740.pdf.%0Ahttps://www.nrel.gov/docs/fy10osti/72740.pdf.%0Ahttps://www.nrel.gov/docs/fy10osti/72740.pdf.%0Ahttps://www.nrel.gov/docs/fy10osti/72740.pdf

Moon, P., Sandí, G., Stevens, D., & Kizilel, R. (2004). Computational modeling of ionic transport in continuous and batch electrodialysis. *Separation Science and Technology*, *39*(11), 2531–2555. https://doi.org/10.1081/SS-200026714

Mubita, T., Porada, S., Aerts, P., & van der Wal, A. (2020). Heterogeneous anion exchange membranes with nitrate selectivity and low electrical resistance. *Journal of Membrane Science*, *607*, 118000. https://doi.org/10.1016/j.memsci.2020.118000

Nie, X. Y., Sun, S. Y., Song, X., & Yu, J. G. (2017). Further investigation into lithium recovery from salt lake brines with different feed characteristics by electrodialysis. *Journal of Membrane Science*, *530*(September 2016), 185–191.

https://doi.org/10.1016/j.memsci.2017.02.020

Noel Jacob, K., Senthil Kumar, S., Thanigaivelan, A., Tarun, M., & Mohan, D. (2014). Sulfonated polyethersulfone-based membranes for metal ion removal via a hybrid process. *Journal of Materials Science*, *49*(1), 114–122. https://doi.org/10.1007/s10853-013-7682-1

Oren, Y. (2008). Capacitive deionization (CDI) for desalination and water treatment - past, present and future (a review). *Desalination*, *228*(1–3), 10–29. https://doi.org/10.1016/j.desal.2007.08.005

Pal, S., Mondal, R., Guha, S., Chatterjee, U., & Jewrajka, S. K. (2019). Homogeneous phase crosslinked poly(acrylonitrile-co-2-acrylamido-2-methyl-1-propanesulfonic acid) conetwork cation exchange membranes showing high electrochemical properties and electrodialysis performance. *Polymer*, *180*(May), 121680. https://doi.org/10.1016/j.polymer.2019.121680

Pang, X., Tao, Y., Xu, Y., Pan, J., Shen, J., & Gao, C. (2020). Enhanced monovalent selectivity of cation exchange membranes via adjustable charge density on functional layers. *Journal of Membrane Science*, *595*(September 2019), 117544. https://doi.org/10.1016/j.memsci.2019.117544

Patel, S. K., Qin, M., Walker, W. S., & Elimelech, M. (2020). Energy Efficiency of Electro-Driven Brackish Water Desalination: Electrodialysis Significantly Outperforms Membrane Capacitive Deionization. *Environmental Science and Technology*, *54*(6), 3663–3677. https://doi.org/10.1021/acs.est.9b07482

Pérez, G., Gómez, P., Ortiz, I., & Urtiaga, A. (2022). Techno-economic assessment of a membrane-based wastewater reclamation process. *Desalination*, *522*. https://doi.org/10.1016/j.desal.2021.115409

Pismenskaya, N. D., Pokhidnia, E. V., Pourcelly, G., & Nikonenko, V. V. (2018). Can the

electrochemical performance of heterogeneous ion-exchange membranes be better than that of homogeneous membranes? *Journal of Membrane Science*, *566*(August), 54–68. https://doi.org/10.1016/j.memsci.2018.08.055

Pushkareva, I. V., Pushkarev, A. S., Grigoriev, S. A., Modisha, P., & Bessarabov, D. G. (2020). Comparative study of anion exchange membranes for low-cost water electrolysis. *International Journal of Hydrogen Energy*, *45*(49), 26070–26079. https://doi.org/10.1016/j.ijhydene.2019.11.011

Radmanesh, F., Rijnaarts, T., Moheb, A., Sadeghi, M., & de Vos, W. M. (2019). Enhanced selectivity and performance of heterogeneous cation exchange membranes through addition of sulfonated and protonated Montmorillonite. *Journal of Colloid and Interface Science*, *533*, 658–670. https://doi.org/10.1016/j.jcis.2018.08.100

Rahimpour, A., Madaeni, S. S., Ghorbani, S., Shockravi, A., & Mansourpanah, Y. (2010). The influence of sulfonated polyethersulfone (SPES) on surface nano-morphology and performance of polyethersulfone (PES) membrane. *Applied Surface Science*, *256*(6), 1825–1831. https://doi.org/10.1016/j.apsusc.2009.10.014

Reahl, A. E. R. (2006). *Half A Century of Desalination With Electrodialysis*.

Rehman, D., Ahdab, Y. D., & Lienhard, J. H. (2019). Improving groundwater quality for irrigation using Monovalent Selective Electrodialysis. *IDA World Congress on Desalination and Water Reuse, Dubai, U.A.E* .

Rehman, D., Ahdab, Y. D., & V, J. H. L. (2021). Monovalent selective electrodialysis: modelling multi-ionic transport across selective membranes. *Water Research*, 117171. https://doi.org/10.1016/j.watres.2021.117171

Ryu, J., Seo, J. Y., Choi, B. N., Kim, W. J., & Chung, C. H. (2019). Quaternized chitosan-based

anion exchange membrane for alkaline direct methanol fuel cells. *Journal of Industrial and Engineering Chemistry*, *73*, 254–259. https://doi.org/10.1016/j.jiec.2019.01.033

Sadrzadeh, M., & Mohammadi, T. (2009). Treatment of sea water using electrodialysis: Current efficiency evaluation. *Desalination*, *249*(1), 279–285. https://doi.org/10.1016/j.desal.2008.10.029

Sharma, P. P., Gahlot, S., & Kulshrestha, V. (2017). One Pot Synthesis of PVDF Based Copolymer Proton Conducting Membrane by Free Radical Polymerization for Electro-Chemical Energy Applications. *Colloids and Surfaces A: Physicochemical and Engineering Aspects*, *520*, 239–245. https://doi.org/10.1016/j.colsurfa.2017.01.088

Sharma, P. P., Gahlot, S., Rajput, A., Patidar, R., & Kulshrestha, V. (2016). Efficient and Cost Effective Way for the Conversion of Potassium Nitrate from Potassium Chloride Using Electrodialysis. *ACS Sustainable Chemistry and Engineering*, *4*(6), 3220–3227. https://doi.org/10.1021/acssuschemeng.6b00248

Sharma, P. P., Yadav, V., Rajput, A., & Kulshrestha, V. (2018). Synthesis of Chloride-Free Potash Fertilized by Ionic Metathesis Using Four-Compartment Electrodialysis Salt Engineering. *ACS Omega*, *3*(6), 6895–6902. https://doi.org/10.1021/acsomega.8b01005

Sharma, P., & Shahi, V. K. (2020). Assembly of MIL-101(Cr)-sulphonated poly(ether sulfone) membrane matrix for selective electrodialytic separation of Pb2+ from mono-/bi-valent ions. *Chemical Engineering Journal*, *382*(September 2019), 122688. https://doi.org/10.1016/j.cej.2019.122688

Shukla, G., Pandey, R. P., & Shahi, V. K. (2016). Temperature resistant phosphorylated graphene oxide-sulphonated polyimide composite cation exchange membrane for water desalination with improved performance. *Journal of Membrane Science*, *520*, 972–982.

https://doi.org/10.1016/j.memsci.2016.08.050

Sinha, M. K., & Purkait, M. K. (2015). Preparation of fouling resistant PSF flat sheet UF membrane using amphiphilic polyurethane macromolecules. *Desalination*, *355*, 155–168. https://doi.org/10.1016/j.desal.2014.10.017

Strathmann, H. (2004). Assessment of Electrodialysis Water Desalination Process Costs. *Proceedings of the International Conference on Desalination Costing, Lemassol, Cyprus, December 6-8, 2004*, *January 2004*, 32–54.

Strathmann, H. (2010). Electrodialysis, a mature technology with a multitude of new applications. *Desalination*, *264*(3), 268–288. https://doi.org/10.1016/j.desal.2010.04.069

Strathmann, H., Krol, J. J., Rapp, H. J., & Eigenberger, G. (1997). Limiting current density and water dissociation in bipolar membranes. *Journal of Membrane Science*, *125*(1), 123–142. https://doi.org/10.1016/S0376-7388(96)00185-8

Takagi, R., Vaselbehagh, M., & Matsuyama, H. (2014). Theoretical study of the permselectivity of an anion exchange membrane in electrodialysis. *Journal of Membrane Science*, *470*, 486–493. https://doi.org/10.1016/j.memsci.2014.07.053

Tavangar, T., Zokaee Ashtiani, F., & Karimi, M. (2020). Morphological and performance evaluation of highly sulfonated polyethersulfone/polyethersulfone membrane for oil/water separation. *Journal of Polymer Research*, *27*(9). https://doi.org/10.1007/s10965-020-02202-5

Thakur, A. K., & Malmali, M. (2022). Advances in polymeric cation exchange membranes for electrodialysis: An overview. *Journal of Environmental Chemical Engineering*, *10*(5), 108295. https://doi.org/10.1016/j.jece.2022.108295

Thakur, A. K., Pandey, R. P., & Shahi, V. K. (2015). Preparation, characterization and thermal

degradation studies of bi-functional cation-exchange membranes. *Desalination*, *367*, 206–215. https://doi.org/10.1016/j.desal.2015.03.037

Unnikrishnan, L., Nayak, S. K., Mohanty, S., & Sarkhel, G. (2010). Polyethersulfone membranes: The effect of sulfonation on the properties. *Polymer - Plastics Technology and Engineering*, *49*(14), 1419–1427. https://doi.org/10.1080/03602559.2010.496399

Vanysek, P. (2012). CRC Handbook of Chemistry and Physics, 93rd Edition, 5–74. 44.

Vaselbehagh, M., Karkhanechi, H., Takagi, R., & Matsuyama, H. (2015). Surface modification of an anion exchange membrane to improve the selectivity for monovalent anions in electrodialysis - experimental verification of theoretical predictions. *Journal of Membrane Science*, *490*, 301–310. https://doi.org/10.1016/j.memsci.2015.04.014

Walker, W. S., Kim, Y., & Lawler, D. F. (2014). Treatment of model inland brackish groundwater reverse osmosis concentrate with electrodialysis-Part I: Sensitivity to superficial velocity. *Desalination*, *344*, 152–162. https://doi.org/10.1016/j.desal.2014.03.035

Wang, X., Zhang, X., Wu, C., Han, X., & Xu, C. (2020). Anion exchange membranes with excellent monovalent anion perm-selectivity for electrodialysis applications. *Chemical Engineering Research and Design*, *158*, 24–32. https://doi.org/10.1016/j.cherd.2020.03.021

White, G. F. (1993). *World_Watershed_Re.Pdf*.

White, N., Misovich, M., Alemayehu, E., Yaroshchuk, A., & Bruening, M. L. (2016). Highly selective separations of multivalent and monovalent cations in electrodialysis through Nafion membranes coated with polyelectrolyte multilayers. *Polymer*, *103*, 478–485. https://doi.org/10.1016/j.polymer.2015.12.019

White, N., Misovich, M., Yaroshchuk, A., & Bruening, M. L. (2015). Coating of Nafion membranes with polyelectrolyte multilayers to achieve high monovalent/divalent cation

electrodialysis selectivities. *ACS Applied Materials and Interfaces*, *7*(12), 6620–6628. https://doi.org/10.1021/am508945p

Wu, S., Cheng, Y., Ma, J., Huang, Q., Dong, Y., Duan, J., Mo, D., Sun, Y., Liu, J., & Yao, H. (2021). Preparation and ion separation properties of sub-nanoporous PES membrane with high chemical resistance. *Journal of Membrane Science*, *635*(May), 119467. https://doi.org/10.1016/j.memsci.2021.119467

Xu, X., He, Q., Ma, G., Wang, H., Nirmalakhandan, N., & Xu, P. (2018). Selective separation of mono- and di-valent cations in electrodialysis during brackish water desalination: Bench and pilot-scale studies. *Desalination*, *428*(June 2017), 146–160. https://doi.org/10.1016/j.desal.2017.11.015

Yang, S. C., Choi, Y. W., Choi, J., Jeong, N., Kim, H., Jeong, H., Byeon, S. Y., Yoon, H., & Kim, Y. H. (2019). Green fabrication of pore-filling anion exchange membranes using R2R processing. *Journal of Membrane Science*, *584*(May), 181–190. https://doi.org/10.1016/j.memsci.2019.04.075

Yun, Y., Tian, Y., Shi, G., Li, J., & Chen, C. (2006). Preparation, morphologies and properties for flat sheet PPESK ultrafiltration membranes. *Journal of Membrane Science*, *270*(1–2), 146–153. https://doi.org/10.1016/j.memsci.2005.06.050

Zhao, J., Guo, L., & Wang, J. (2018). Synthesis of cation exchange membranes based on sulfonated polyether sulfone with different sulfonation degrees. *Journal of Membrane Science*, *563*(January), 957–968. https://doi.org/10.1016/j.memsci.2018.05.023

Zhao, J., Ren, L., Chen, Q. bai, Li, P., & Wang, J. (2020). Fabrication of cation exchange membrane with excellent stabilities for electrodialysis: A study of effective sulfonation degree in ion transport mechanism. *Journal of Membrane Science*, *615*(July), 118539.

https://doi.org/10.1016/j.memsci.2020.118539

Zhao, J., Sun, L., Chen, Q., Lu, H., & Wang, J. (2019). Modification of cation exchange membranes with conductive polyaniline for electrodialysis applications. *Journal of Membrane Science*, *582*(October 2018), 211–223. https://doi.org/10.1016/j.memsci.2019.03.043

Zhao, Y., Li, Y., Yuan, S., Zhu, J., Houtmeyers, S., Li, J., Dewil, R., Gao, C., & Van Der Bruggen, B. (2019). A chemically assembled anion exchange membrane surface for monovalent anion selectivity and fouling reduction. *Journal of Materials Chemistry A*, *7*(11), 6348–6356. https://doi.org/10.1039/c8ta11868j

Zhao, Y., Qiu, Y., Mai, Z., Ortega, E., Shen, J., Gao, C., & Van Der Bruggen, B. (2019). Symmetrically recombined nanofibers in a high-selectivity membrane for cation separation in high temperature and organic solvent. *Journal of Materials Chemistry A*, *7*(34), 20006–20012. https://doi.org/10.1039/c9ta07416c

Zhu, H., Yang, B., Gao, C., & Wu, Y. (2020). Ion transfer modeling based on Nernst–Planck theory for saline water desalination during electrodialysis process. *Asia-Pacific Journal of Chemical Engineering*, *15*(2), 1–11. https://doi.org/10.1002/apj.2410

Zhu, J., Liao, J., Jin, W., Luo, B., Shen, P., Sotto, A., Shen, J., & Gao, C. (2019). Effect of functionality of cross-linker on sulphonated polysulfone cation exchange membranes for electrodialysis. *Reactive and Functional Polymers*, *138*(March), 104–113. https://doi.org/10.1016/j.reactfunctpolym.2019.02.006

Zhu, J., Luo, B., Qian, Y., Sotto, A., Gao, C., & Shen, J. (2019). Three-Dimensional Stable Cation-Exchange Membrane with Enhanced Mechanical, Electrochemical, and Antibacterial Performance by in Situ Synthesis of Silver Nanoparticles. *ACS Omega*, *4*(15), 16619–16628.

https://doi.org/10.1021/acsomega.9b02537

Zourmand, Z., Faridirad, F., Kasiri, N., & Mohammadi, T. (2015). Mass transfer modeling of desalination through an electrodialysis cell. *Desalination*, *359*, 41–51. https://doi.org/10.1016/j.desal.2014.12.008

Curriculum Vita

Li Chen obtained his Bachelor of Engineering degree in Hohai University, Nanjing, China in 2012. After three years' study, he obtained his Master of Engineering degree in Environmental Engineering in Shanghai Polytechnic University, Shanghai, China in 2018. During the application of his PhD program at University of Texas at El Paso (UTEP), he had one year industry work experience, which was related to the research and application of pervaporation membranes. He started his PhD program in 2019 and was supported by funding from the Nano systems Engineering Research Center for Nanotechnology-Enabled Water Treatment (NEWT). His research included ion exchange membranes fabrication and electrodialysis desalination performance tests. Additionally, he participated in an industrial internship with Carollo Engineers consulting firm in Phoenix, AZ to assist the development team of Blue Plan-it® (a water industry decision-making software). Eventually, Li Chen's hope is to contribute to society with his talents and skills to make the earth a better place.

Contact Information: li.chen20111021@gmail.com

Web: linkedin.com/in/li-chen-b17668197